AD_____

Award Number: DAMD17-02-1-0095

TITLE: Hyaluronic Acid and Hyaluronidase in Prostate Cancer: Evaluation of Their Therapeutic and Prognostic Potential

PRINCIPAL INVESTIGATOR: Vinata B. Lokeshwar, Ph.D.

CONTRACTING ORGANIZATION: University of Miami School of Medicine
Miami, Florida 33136

REPORT DATE: January 2003

TYPE OF REPORT: Annual

PREPARED FOR: U.S. Army Medical Research and Materiel Command
Fort Detrick, Maryland 21702-5012

REPORT DOCUMENTATION PAGE

Form Approved
OMB No. 074-0188

1. AGENCY USE ONLY (Leave blank)	2. REPORT DATE	3. REPORT TYPE AND DATES COVERED
	January 2003	Annual (1 Jan 02 - 31 Dec 02)

4. TITLE AND SUBTITLE
Hyaluronic Acid and Hyaluronidase in Prostate Cancer: Evaluation of Their Therapeutic and Prognostic Potential

5. FUNDING NUMBERS
DAMD17-02-1-0095

6. AUTHOR(S) :
Vinata B. Lokeshwar, Ph.D.

7. PERFORMING ORGANIZATION NAME(S) AND ADDRESS(ES)
University of Miami School of Medicine
Miami, Florida 33136

E-Mail: vlokeshw@med.miami.edu

8. PERFORMING ORGANIZATION REPORT NUMBER

9. SPONSORING / MONITORING AGENCY NAME(S) AND ADDRESS(ES)
U.S. Army Medical Research and Materiel Command
Fort Detrick, Maryland 21702-5012

10. SPONSORING / MONITORING AGENCY REPORT NUMBER

11. SUPPLEMENTARY NOTES
Original contains color plates: All DTIC reproductions will be in black and white.

12a. DISTRIBUTION / AVAILABILITY STATEMENT
Approved for Public Release; Distribution Unlimited

12b. DISTRIBUTION CODE

13. Abstract ***(Maximum 200 Words)*** *(abstract should contain no proprietary or confidential information)*

The limited knowledge about which clinically localized prostate cancer (CaP) would progress, and when it will recur severely impedes individualization of therapy and prediction of outcome. Several molecules that function in cancer growth and progression can serve as prognostic indicators. Treatment modalities that target the functions of these molecules could effectively control CaP progression. We have studied two such molecules, hyaluronic acid (HA) and HYAL1 type hyaluronidase (HAase). HA is a glycosaminoglycan and HAase is an enzyme that degrades HA into angiogenic fragments. Immunohistochemical analysis using archival radical prostatectomy CaP specimens, from patients on whom there is minimum 5-year follow-up, show that HYAL1 and combined HA-HYAL1 staining are independent predictors for biochemical recurrence. Patients with high HA-HYAL1 staining in their CaP tissues have an 18-fold increased risk of biochemical recurrence within 5-years, regardless of other clinical and pathologic parameters. Studies on functional analysis of HYAL1 using 3 HAase inhibitors show that inhibition of HAase activity also inhibits CaP cell proliferation. The degree of inhibition of cell proliferation is dependent on the degree of inhibition of HAase activity. Ongoing studies are examining the effect of HAase inhibition (i.e., using antisense cDNA transfection or HAase inhibitors) on CaP growth and progression *in vivo*.

14. SUBJECT TERMS:	15. NUMBER OF PAGES
growth, progression, prognosis, therapy, hyaluronidase, hyaluronic acid, prostate cancer	37
	16. PRICE CODE

17. SECURITY CLASSIFICATION OF REPORT	18. SECURITY CLASSIFICATION OF THIS PAGE	19. SECURITY CLASSIFICATION OF ABSTRACT	20. LIMITATION OF ABSTRACT
Unclassified	Unclassified	Unclassified	Unlimited

Table of Contents

Principal Investigator: Vinata B. Lokeshwar, Ph.D.

Project Title: Hyaluronic acid and hyaluronidase in prostate cancer: Evaluation of their therapeutic and prognostic potential.

A. Introduction and objectives: There are two overall objectives of this funded project. The first is to evaluate the independent prognostic potential of two tumor markers, identified in our laboratory, i.e., hyaluronic acid (HA) and HYAL1 type hyaluronidase (HAase). The second objective is to evaluate the effect of HYAL1 inhibition on prostate cancer (CaP) growth and metastasis using two complementary approaches, i.e., the antisense approach and the use of a HAase inhibitor, VERSA-TL 502. We also plan to examine the mechanism by which HYAL1 regulates CaP cell growth and metastasis.

The majority of the newly diagnosed prostate cancer (CaP) patients have clinically organ-confined disease. However, limited knowledge about which CaP is likely to progress, as well as, when it will recur severely impedes individualized selection of therapy and subsequent prediction of outcome (1-5). Advances in tumor biology have unraveled genes and their products that closely associate and function in CaP growth, metastasis and angiogenesis (1,6-8). Some of the molecules may serve as accurate prognostic indicators. Moreover, treatment modalities that target the functions of these molecules could effectively control CaP progression. In preliminary studies we identified that HA and HYAL1 type HAase may be such markers. HA is a glycosaminoglycan that is made up of repeating disaccharide units, D-glucuronic acid and N-acetyl-D-glucosamine. It is abundantly present in tissues and tissue fluids. In addition to its structural role, HA regulates several cellular processes (9-10). Concentrations of HA are elevated in several cancers including those of colon, breast and in bladder (11-19). In a published report that we had presented as the preliminary evidence at the time of submission of this funded project, we demonstrated that HA levels are 4-8-fold elevated in CaP tissues, when compared to the normal prostate and benign prostatic hyperplasia tissues (20). Immunohistochemical analysis demonstrated that HA present in CaP tissues mostly localizes to the tumor-associated stroma. Small fragments of HA are known to be anigogenic and we showed the presence of such angiogenic HA fragments in high-grade CaP tissues.

HAase is an endoglycosidase that cleaves internal β-N-acetyl-D-glucosaminic linkages in the HA polymer, yielding HA fragments (21). At present 6 HAase genes have been identified, which cluster into two tightly linked triplets on chromosomes 3p21.3 (HYAL1, HYAL2 and HYAL3) and 7q31.3 (HYAL4, PH20, HYALp1) (22). Using RT-PCR, cDNA cloning/sequencing, cell-culture, immunoblotting and pH activity profile studies, we confirmed that HYAL1 is the HAase that is expressed in CaP tissues and it is secreted by CaP cells (23). We also showed that HAase levels are elevated in CaP tissues when compared to the levels in NAP and BPH tissues. Furthermore, the increase in HAase levels correlates with CaP progression (metastatic > high-grade >> low-grade (Gleason 5/6) > NAP/BPH) (23). By immunohistochemical analysis, which was presented as the preliminary evidence during the submission of this funded project, we showed that the HYAL1 type HAase is exclusively expressed in CaP cells. Based on our immunoshistochemical studies we hypothesized that HA and HYAL1 may be potentially accurate prognostic indicators for CaP. To investigate the function of HYAL1 we had stablely transfected DU145 cells with full-length HYAL1 cDNA in the sense and antisense orientation. We found that transfection of HYAL1 cDNA in the antisense orientation decreased cell growth (4-fold), induced a G2/M block in the cell cycle and caused a 50% inhibition of Matrigel™ invasion when compared to both vector only and HYAL1-sense transfectants. We proposed to test the behavior of HYAL1 transfectants *in vivo* (tumor growth and metastasis studies). In addition, we had identified a HAase inhibitor, VERSA-TL502 (24). This inhibitor inhibits the HAase activity secreted by CaP cells (IC_{50} 2 μg/ml). Since blocking the expression of HYAL1

results in decreased CaP cell growth we had hypothesized that VERSA-TL 502 may also inhibit CaP cell growth and invasive behavior, both *in vitro* and *in vivo*.

The following is a succinct report of the progress in achieving our objectives in the first year of the three-year project.

B. Progress related to Aim 1: To correlate HA and HYAL1 staining intensity and its pattern in CaP tissues with clinical outcome.

B.1 Experimental procedures:

Specimens and study individuals: We initially chose 150 archival specimens from CaP patients who underwent retropubic prostatectomy for clinically localized CaP between 1992 and 1996. Out of these 150 patients, on 73 patients, a minimum 5-year follow-up was available. Three out of the total 73 specimens were not included in the final analysis since those patients had positive lymph nodes. Out of the 70 patients included in the final analysis, the progressed group of patients (n = 25) includes those who had biochemical recurrence (PSA > 0.4 ng/ml) within 64 months (mean time to recurrence = 21.3 months; range 3 to 61 months). The non-progressed group includes patients (n = 45) who were disease free (i.e., no clinical or biochemical recurrence) for a minimum of 64 months (mean follow-up 80.6 months; range 64 – 114 months). The patient characteristics with respect to age, pre-operative PSA and tumor (i.e., Gleason, stage, margin, EPE, seminal vesicle invasion) are shown in Table 1.

Table 1: Distribution of pre- and post-operative parameters among study patients. Note that biochemical recurrence with post-operative PSA levels ≥ 0.4 ng/ml within 64 months was used a cut point for defining progression. Thus, any CaP patient who showed a biochemical recurrence within 64 months was included in the progressed category.

	Age (Years)	PSA (ng/ml)	Clinical Stage	Gleason Sum	EPE	Margin	Seminal Vesicle Invasion
Biochemical recurrence (n = 25)	Median: 64 Mean: 65.1 Range: 51-74	Median: 9.0 Mean: 14.04 Range:2- 62	T1 C = 10 T2 A = 5 T2 B = 10	6 = 2 7 = 14 8 = 6 9 = 3	(+) = 21 (-) = 4	(+) = 18 (-) = 7	(+) = 14 (-) = 11
No biochemical or clinical recurrence (n = 45)	Median: 65 Mean: 63.5 Range: 40-75	Median: 6.0 Mean: 7.9 Range: 0.5 - 23	T1 C = 24 T2 A = 6 T2 B = 15	5 = 8 6 = 9 7 = 22 8 = 6	(+) = 6 (-) = 39	(+) = 10 (-) = 35	(+) = 3 (-) = 42

HA and HYAL1 staining: IHC localization of HA and HYAL1 in CaP tissues was carried out as described previously (20). For all specimens, paraffin-embedded blocks containing CaP tissues representing the majority of the Gleason sum were selected by the study 's pathologist (Dr. Francisco Civantos). The blocks were cut into 3-μm thick sections and placed on positively charged slides. The specimens were deparafinized, rehydrated and treated with an Antigen-retrieval solution (Dako Laboratories). For each specimen, two slides were prepared, one for HA and the other for HYAL1 staining. For HA staining, the slides were incubated with 2 μg/ml of a biotinylated bovine nasal cartilage protein at room temperature for 35 min (20). The specificity of HA staining was established as described previously (20). Following incubation with the HA-

binding protein, the slides were washed in phosphate buffered saline (PBS) and sequentially incubated with streptavidin peroxidase at room temperature for 30 min and 3,3-diaminobenzidine (DAB) chromogen substrate solution (Dako Laboratories). The slides were counterstained with hematoxylin, dehydrated and mounted.

For HYAL1 staining, the slides were incubated with 3.7 μg/ml of anti-HYAL1 IgG at 4^0 C for 16 hr. Rabbit polyclonal anti-HYAL1 IgG was generated against a peptide sequence present in HYAL1 protein (amino acids 321 to 338) and its specificity for IHC was confirmed as described previously (20, 25). Following incubation with anti-HYAL1 IgG, the slides were washed in PBS and incubated with a linking solution containing a biotinylated goat anti-rabbit IgG (Dako LSAB kit) at room temperature for 30 min. The slides were then treated with streptavidin peroxidase and DAB chromogen. The slides were counterstained with hematoxylin, dehydrated and mounted.

Slide grading: Two readers independently evaluated all slides in a blinded fashion. Any discrepancy in assigning staining intensity was resolved by both readers reexamining those slides simultaneously. The staining for HA and HYAL1 was graded as 0 (no staining), 1+, 2+ and 3+. For HA staining, in each slide, both the tumor-associated stroma and tumor cells were graded separately for staining intensity. In case of HA staining, the stromal staining was also evaluated as dense or sparse. The overall staining grade for each slide was assigned based on the staining intensity of the majority of the tumor tissue in the specimen. However, if approximately 50% of the tumor tissue stained as 1+ and the other 50% as 3+, the overall staining grade was 2+. If the staining distribution was, approximately 50% of the tumor staining 2+ and the remaining staining as 3+, the overall staining inference was assigned as 3+. The staining scale was further subcategorized into low-grade and high-grade.

For HA staining, low-grade includes 0, 1+ sparse and 2+ sparse/dense staining and high-grade staining includes 3+ sparse and 3+ dense staining. In those cases (n=2), where the stromal tissues were evaluated as low-grade staining but the tumor cells stained as 3+, the overall HA staining was considered as high-grade. For HYAL1, high-grade staining represents, 2+ and 3+ staining, whereas, low-grade staining includes 0 and 1+ staining intensities. For the combined HA-HYAL1 staining, a positive result was indicated only when both HA (stromal, tumor cells or both) and HYAL1 staining intensities were of high-grade. Any other combination was considered as negative.

High-grade staining was considered as a true positive result and the low-grade staining indicated a false negative result if the patient had biochemical recurrence. If the patient had no clinical/biochemical recurrence, the low-grade staining indicated a true negative result and the high-grade staining, was taken as a false positive result.

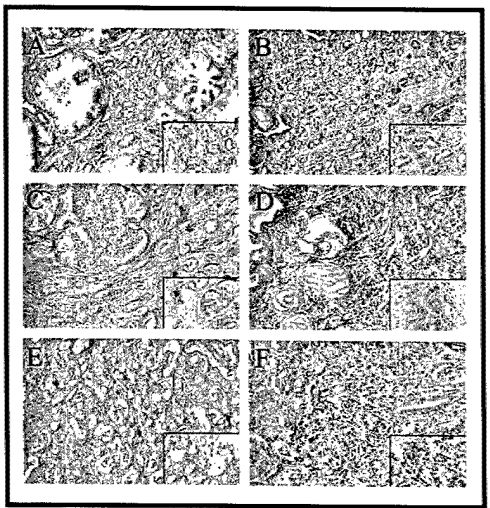

Figure 1. HA staining of CaP specimens from non-progressed and progressed patients. Panels A, C and E: HA staining in specimens from non-progressed patients. Panels B, D and F: HA staining in specimens from progressed patients. A, B: Gleason 6 CaP; C, D: Gleason 7 CaP; E, F: Gleason 8 CaP.

Results:

HA localization: Fig. 1 shows HA staining in Gleason sum 6 (A, B) 7 (C, D) and 8 (E, F) CaP specimens from non-progressed (A, C, E) and progressed (B, D, F) patients. In all of the CaP specimens HA is localized mostly in the tumor-associated stroma, although some tumor cells also show HA staining in CaP specimens from patients who progressed (panels B and F). As shown in Fig. 1 A, C, and E the CaP specimens from

Figure 2: A Gleason 8 CaP specimen with tumor cells showing HA staining. Gleason 8 specimen from a progressed patient where tumor cells show high-grade HA staining. A: 100 X magnification. B: 400 X magnification.

non-progressed patients have low-grade HA staining, regardless of the Gleason sum. Out of the 45 patients free of recurrence, 26 had low-grade HA staining. However, the CaP specimens from the patients who progressed in < 64 months (median time to recur = 19 months; mean time to recur = 21.3 months), show high-grade HA staining (Panels B, D, F). Out of the 25 CaP specimens from progressed patients, 22 showed high-grade staining in tumor stroma; 8 of these 22 also showed high-grade HA staining in tumor cells. In addition, 2 of the 25 CaP specimens showed high-grade staining only in tumor cells. Fig. 2 shows an example of tumor cells that are positive for high-grade HA staining. Tumors cells appear to stain for HA equally, both in the cytoplasm and plasma membrane (Fig. 2 B, magnified view). Thus, out of the 25 CaP specimens from progressed patients, 24 showed high-grade HA staining either in tumor stroma, tumor cells or both. Thus, high-grade HA staining (stroma, tumor cells or both) has 96% sensitivity, 55.5% specificity, 70% accuracy, 54.5% PPV and 96.2% NPV for predicting the biochemical recurrence (Table 2).

Table 2: Sensitivity, specificity, accuracy, PPV and NPV of HA, HYAL1 and combined HA-HYAL1 staining inferences for predicting biochemical recurrence in CaP patients. Note that 64 month follow-up was used a cut point for determining biochemical recurrence. Please note that 2 of the CaP patients who had a biochemical recurrence at 70 months and showed high-grade HA, HYAL1 and combined HA-HYAL1 staining were considered as false-positives and were included in the specificity calculation.

Parameters	HA	HYAL1	HA-HYAL1
Sensitivity	96% (24/25)	84% (21/25)	84% (21/25)
Specificity	55.5% (25/45)	82.2% (37/45)	86.7% (39/45)
Accuracy	70% (49/70)	82.9% (58/70)	85.7% (60/70)
PPV	54.5% (24/44)	70% (21/30)	77.8% (21/27)
NPV	96.2% (25/26)	90.2% (37/41)	90.7% (39/43)

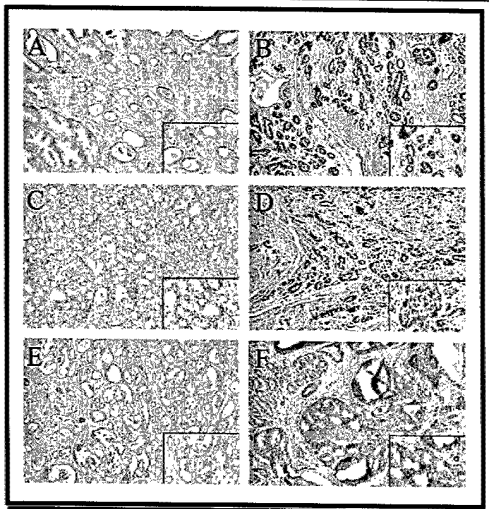

HYAL1 localization: Fig. 3 shows HYAL1 localization in Gleason 6 (A, B), 7 (C, D) and 8 (E, F) CaP tissues from patients who did not (A, C, E) and who did (B, D, F) progress. As shown in Fig. 3, low-grade HYAL1staining is seen in all 3 CaP specimens from patients who did not progress, regardless of their Gleason sum (Fig. 3, panels A, C and E). Among the 45 non-progressed patients, Cap specimens of 36 patients showed low-grade HYAL1 staining. In CaP specimens from progressed patients, tumor cells, and not tumor-stroma, stain for HYAL1. All 3 CaP specimens from progressed patients show high-grade HYAL1 staining (Fig. 3, panels B, D and F), regardless of their Gleason sum.

Figure 3: HYAL1 staining of CaP specimens from non-progressed and progressed patients. Panels A, C and E: HYAL1 staining in specimens from non-progressed patients. Panels B, D and F: HYAL1 staining in specimens from progressed patients. A, B: Gleason 6 CaP; C, D: Gleason 7 CaP; E, F: Gleason 8 CaP.

Out of the 25 progressed patients, CaP specimens from 21 patients showed high-grade HYAL1 staining. Thus, in this cohort of 70 patients, the HYAL1 localization in CaP specimens has 84% sensitivity, 82.2% specificity, 82.9% accuracy, 70% PPV and 90.2% NPV for predicting biochemical recurrence within 64 months (Table 2).

Combined HA-HYAL1 staining: We next determined the ability of combined high-grade HA and HYAL1 staining to predict biochemical recurrence. The combined HA-HYAL1 staining has 84% sensitivity, 86.7% specificity, 85.7% accuracy, 77.8% PPV and 90.7% NPV for predicting progression. When 64 months was used as a cut-off limit to evaluate progression, there were 7 false positive cases, i.e., the specimens showed high-grade HA and HYAL1 staining but the patients had no disease recurrence within 64 months. However, among these 7 false positive cases, 2 had a biochemical recurrence at 70 months (Table 2).

Evaluation of the prognostic capabilities of pre-operative, post-operative parameters and HA and HYAL1 staining inferences:

Univariate analysis: We performed a univariate logistic regression analysis to determine the prognostic significance of pre-operative parameters (i.e., age, PSA and clinical stage), post-operative surgical and pathologic parameters (i.e., Gleason sum, margin +/-, EPE, seminal vesicle invasion +/-), as well as, inferences of HA, HYAL1 and combined HA-HYAL1 staining. As shown in Table 3, both age (P= 0.297; odds ratio (OR) = 1.041) and stage (P = 0.287; OR = 1.714) are not significant in predicting biochemical recurrence in the univariate analysis. However, pre-operative PSA (P = 0.0174; OR = 1.10), Gleason sum (P = 0.0023; OR = 3.062); positive margin (P = 0.0001; OR = 9.0), EPE (P < 0.0001; OR = 34.125), seminal vesicle invasion (P <0.0001; OR = 17.818), HA staining (P = 0.0014, OR = 30), HYAL1 staining (P < 0.0001; OR = 24.28) and combined HA-HYAL1 staining (P < 0.0001; OR = 34.125) are found to be significant in predicting biochemical recurrence. Patients with Gleason sum $\geq$ 7 have been shown to have a greater risk of progression (26). In the univariate analysis, Gleason sum $\geq$ 7 patients had 2.3-fold greater odds of developing biochemical recurrence (P = 0.015; OR = 6.982) than when CaP tissues all Gleason sums were analyzed together (Table 3).

Table 3: Univariate analysis of pre- and post-operative prognostic parameters and HA, HYAL1 and combined HA-HYAL1 staining inferences. *: Statistically significant. CI: Confidence Interval.

Parameter	*Chi* square	P value	Odds Ratio	95% CI
Age	1.088	0.297	1.041	0.965 – 1.122
PSA	5.652	0.0174*	1.1	1.017 – 1.192
Clinical stage	0.539	0.287	1.741	0.636 – 4.621
Gleason sum (Overall)	9.266	0.0023*	3.062	1.49 – 6.294
Gleason sum $\geq$ 7	5.919	0.015*	6.982	1.459 – 33.411
Margin	14.764	0.0001*	9.0	2.934 – 27.603
EPE	25.435	< 0.0001*	34.125	8.655 – 134.545
Seminal vesicle invasion	15.969	< 0.0001*	17.818	4.339 – 73.175
HA	10.222	0.0014*	30.0	3.729 – 241.337
HYAL1	22.627	< 0.0001*	24.281	6.524 – 90.375
HA-HYAL1	25.435	< 0.0001*	34.125	8.655 – 134.545

Forward stepwise multiple logistic regression analysis: To determine the smallest number of variables that can jointly predict biochemical recurrence in this cohort of study patients, we performed the forward stepwise multiple logistic regression analysis. Initially, when age, pre-

operative PSA, clinical stage, Gleason sum, EPE, seminal vesicle invasion, HA staining and HYAL1 staining were included in the model, only EPE (P = 0.0023; OR = 33.483), positive margin (P = 0.0059; OR = 26.948), HYAL1 staining (P = 0.0094; OR = 12.423) reached statistical significance in predicting biochemical recurrence (Table 4 a). Gleason sum did not reach statistical significance in the multiple logistic regression analysis even after the patients were stratified according to Gleason ≥ 7 and < 7 (data not shown).

The inclusion of the combined HA-HYAL1 staining inference instead of the individual HA and HYAL1 staining inferences, in the multiple regression model, again showed that EPE (P = 0.0023; OR = 35.944), margin (P = 0.0086; OR = 24.438) and HA-HYAL1 staining (P = 0.0033; OR = 18.047) were significant in predicting biochemical recurrence. None of the other routine prognostic parameters (i.e., age, PSA, clinical stage, Gleason sum (or Gleason stratification as Gleason ≥ 7 and < 7 and seminal vesicle invasion) that were included in the model reached statistical significance (i.e., P > 0.05 in each case).

Table 4: Forward stepwise multiple logistic regression analysis of pre- and post-operative prognostic parameters and HA, HYAL1 and combined HA-HYAL1 staining inferences. The significant parameters (P > 0.05) selected by the model are shown. **A:** In the analysis, HA and HYAL1staining inferences were included separately, along with other pre- (i.e., age, PSA and clinical stage) and post- (i.e., Gleason sum (or stratified Gleason as ≥ 7 and < 7), EPE, margin +/-, and seminal vesicle invasion) surgery parameters. **B:** Combined HA-HYAL1 staining inference was included in the analysis together with the above-mentioned pre- and

	Table 4 A				**Table 4 B**			
Parameter	*Chi* Square	P value	Odds Ratio	95% CI	*Chi* Square	P value	Odds Ratio	95% CI
EPE	15.20	0.0023*	33.483	3.493 – 320.912	9.271	0.0023*	35.944	3.583 – 360.565
Margin	7.573	0.0059*	26.948	2.58 – 281.463	6.895	0.0086*	24.438	2.249 - 265.55
HYAL1	6.846	0.0094*	12.423	1.856 – 83.158	NA	NA	NA	NA
HA-HYAL1	NA	NA	NA	NA	8.628	0.0033*	18.047	2.619 – 124.378

Summary: The results, which we have obtained, demonstrate that HYAL1 and HA-HYAL1 are independent prognostic indicators for predicting biochemical recurrence of CaP. An additional point that deserves attention is that in this study we had a reasonably long follow-up on each patient (a minimum follow-up of > 5 years), which was sufficient to detect any biochemical recurrence. This long follow-up makes a strong case that HYAL1 and HA-HYAL1 are potentially useful prognostic indicators for CaP. In the next phase of the study, we are planning to compare these markers with other tumor markers using the same archival specimens.

C. Progress related to Aim 2: To evaluate the effect of HYAL1 inhibition on CaP growth and metastasis.

C.1 Effect of HAase inhibitors on the HAase activity secreted in DU145 culture conditioned media: In addition to VERSA-TL 502 that we had mentioned in our proposal we

obtained 2 more HAase inhibitors namely T-PSS (Polystyrene sulfonate) and PMHS (Polymethylene hydroquinone sulfonate). Both these inhibitors were kindly provided by Drs. Drs. Anderson and Zaneveld. According to Drs. Zaneveld, T-PSS is as good a inhibitor as VERSA-TL 502 to inhibit the testicular HAase, however, PMHS is a weaker inhibitor.

We compared the ability of these inhibitors to block the HYAL1 type HAase activity secreted in the conditioned media using the HAase test. The **HAase test** is an ELISA-like assay where microtiter plates coated with 200 μg/ml HA are incubated with different samples (e.g., conditioned medium) in an HAase assay buffer (27). Following incubation, the degraded HA is washed off and HA remaining on the wells is detected using a biotinylated HA binding protein and an avidin-biotin detection system. HAase activity (mU/ml) is normalized to total protein and expressed as mU/mg.

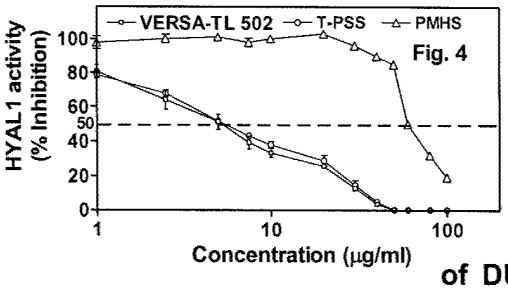

As shown in Fig. 4 both VERSA-TL 502 and T-PSS caused a dose-dependent inhibition of HAase activity present in the conditioned medium of DU145 cells (IC_{50} 5.2 μg/ml). However, PMHS was a weak inhibitor of HAase activity (IC_{50} 60 μg/ml).

C.2 Effect of HAase inhibitors on the growth of DU145 and PC3-ML cells. To test the effect of HAase inhibitors on CaP cell growth, DU145 and PC3-ML cells (1.5 x 10^4 cells/well) were plated on 24-well plates in growth medium in the presence of various concentrations (0-20 μg/ml) of VERSA-TL 502, T-PSS or PMHS. Every 24-hr for 96-hr, cells were stained with trypan blue and counted. As shown in Fig. 5 A and B HAase inhibitors inhibit growth of both DU145 and PC3-ML cells. Furthermore, among the 3 inhibitors, VERSA-TL 502 was the most effective. At 5 μg/ml, IC_{50} for HAase activity, the growth inhibition by VERSA-TL 502 was 61% in DU145 and 86% in PC3-ML cells, when compared to T-PSS (40% HT1376 and 52% 253J-Lung) and PMHS (5% for DU145 and PC3-ML).

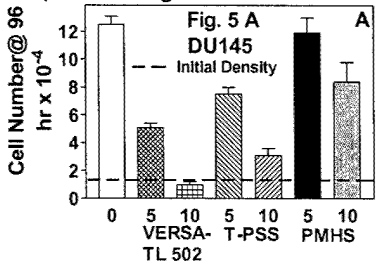

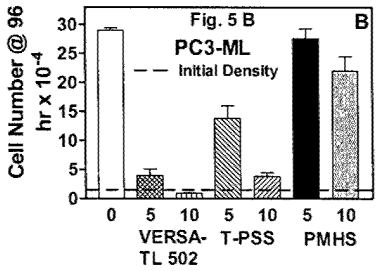

Currently, we are testing the effect of these HAase inhibitors on the invasive properties of DU145 and PC3-ML cells, using the Matrigel™ invasion assay (28).

C.3 Experiments in progress

Examination of the *in vivo* behavior of DU145 transfectants: To study HYAL1 functions *in vivo* (i.e., tumor growth and invasion), we have implanted HYAL1-sense, HYAL1-antisense and vector transfectants of DU145 cells bilaterally (one on each flank) s.c. at 2 x 10^6 cell density per site. We have injected 5 athymic mice on January 15th and are waiting for the tumor to become palpable. Once the tumors become palpable, we will measure tumor size twice-weekly using calipers and calculate tumor volume (length x width x depth x 0.5236) (29). When tumors in the vector only group reach 1 cm^3, the mice will be euthanized and tumors will be weighed and fixed for histology.

Determination of a non-toxic dose of VERSA-TL 502: To determine the non-toxic dose of VERSA-TL 502 for animal studies, we have injected four groups of 5 mice each i.p. with phosphate buffered saline (PBS) or 0.5, 1 and 5 mg of VERSA-TL 502 dissolved in 0.1 ml of PBS. The first injection was done on January 20th. We will be injecting VERSA-TL 502 twice weekly and observe mice for malaise and weight loss for the next six weeks. Once the

maximum tolerated dose is determined, we will use that dose to study the effect of VERSA-TL 502 on tumor growth and metastasis.

Generation of PC3-ML transfectants: We will be starting to generate HYAL1-sene, HYAL1-antisense and vector transfectants of PC3-ML cells in the beginning of February.

Summary: The results that we have obtained so far demonstrate that HAase inhibitors are able to inhibit the growth of CaP cells. But more interestingly, the growth inhibitory activity of HAase inhibitors correlates with the HAase inhibitory activity of these inhibitors. For example, VERSA-TL 502 is a potent inhibitor of HAase activity secreted by CaP cells and it is an effective inhibitor CaP cell proliferation. On the contrary, PMHS, which is a weak inhibitor of HAase activity, causes very little growth inhibition.

2 Key achievements:

A. Archival tissue specimens from CaP patients with a minimum follow-up of 64 months were stained for HA and HYAL1 using immunohistochemistry

B. HA staining alone either in the stroma or tumor cells was significant in predicting biochemical recurrence, but in the multivariate analysis it was not an independent predictor of prognosis.

C. HYAL1 and combined HA-HYAL1 staining inferences proved to be independent prognostic indicators for predicting biochemical recurrence. The odds of a CaP patient will have biochemical recurrence are 12 and 18-fold higher, respectively, if the CaP tissue stains high for HYAL1 or combined HA-HYAL1. This is the **first study**, which demonstrates the prognostic potential of HYAL1 in any type of cancer.

D. Synthetic HAase inhibitors inhibit HAase activity secreted by CaP cells and also inhibit the growth of CaP cells. The growth inhibitory activity of HAase inhibitors correlates with their ability to inhibit HAase activity.

3. Reportable outcomes:

A. Publications: 1. Lokeshwar, V.B. Schroeder, G.L., Carey, R.I. Soloway, M.S., Iida, N. Regulation of hyaluronidase activity by alternative mRNA splicing. J. Biol. Chem. 2002

2. Posey, J.T., Soloway, M.S., Ekici, S., Sofer, M., Civantos, F., Duncan, R.C., Lokeshwar, V.B., Evaluation of the prognostic potential of hyaluronic acid and hyaluronidase (HYAL1) for prostate cancer: A five-year study, 2002 (Submitted to Cancer Research)

B. Patents: No patents were filed or issued.

C. Clinical translational research: No clinical trials were undertaken.

D. Personnel: One full time postdoctoral fellow (September to present), a resident in the department of urology, a pathologist, a statistician and the P.I. worked on this project. One clinical fellow in the department of urology, together with the urologists, provided the clinical information.

4. Conclusions: Results derived from the experiments performed under Aim 1, demonstrate that HYAL1 and HA-HYAL1 are sensitive and specific markers for predicting biochemical recurrence for CaP patients who undergo radical prostatectomy. The multivariate analysis establishes for the first time, the independent prognostic potential of HYAL1 type HAase for any type of cancer, in general and for CaP in particular. The experiments planned in the coming

months will compare the prognostic potential of both HYAL1 and combined HA-HYAL1 with other prognostic indicators, including microvessel density. The experiments conducted under Aim 2, demonstrate that HAase inhibition may halt CaP growth and progression. Since the HAase inhibitors inhibit the growth of CaP cells, it gives support to the hypothesis that an anti-HAase therapy may halt CaP progression. The *in vivo* experiments planned this year should be able to reveal whether anti-HAase therapy has the potential to be useful for CaP.

5. REFERENCES:

1. Pettaway, C.A. Prognostic markers in clinically localized prostate cancer. Tech. Urol., 4: 35-42, 1998.
2. Blute, M.L. Bergstralh, E.J., Iocca, A., Scherer, B., Zincke, H. Use of Gleason score, prostate specific antigenm seminal vesicle and margin status to predict biochemical failure after radical prostatectomy. J. Urol., 165: 119-125, 2001.
3. Muzzonigro, G., Galosi, A.B. Biological selection criteria for radical prostatectomy. Ann N Y Acad Sci. 963:204-212, 2002.
4. Small, E.J., Roach M 3rd. Prostate-specific antigen in prostate cancer: a case study in the development of a tumor marker to monitor recurrence and assess response. Semin Oncol. 29: 264-73, 2002.
5. Palisaan, R.J., Graefen, M., Karakiewicz, P.I., Hammerer, P.G., Huland, E., Haese, A., Fernandez, S., Erbersdobler, A., Henke, R.P., Huland, H. Assessment of clinical and pathologic characteristics predisposing to disease recurrence following radical prostatectomy in men with pathologically organ-confined prostate cancer. Eur Urol. 41:155-161, 2002.
6. Isaacs W, De Marzo A, Nelson W. Focus on prostate cancer. Cancer Cell. 2:113-116, 2002.
7. Muzzonigro, G., Galosi, A.B. Biological selection criteria for radical prostatectomy. Ann N Y Acad Sci. 963:204-212, 2002.
8. Partin, A.W., Murphy, G.P., Brawer, M.K. Report on Prostate Cancer Tumor Marker Workshop 1999. Cancer, 88: 955- 963, 2000.
9.Tool, BP. Hyaluronan is not just a gloo! J. Clin. Invest. 106: 335-336, 2000.
10. Delpech, B., Girard, N., Bertrand, P., Courel, N.M., Chauzy, C., Delpech, A. Hyaluronan: Fundamental principles and applications in cancer. J. Intern. Med. 242: 41-48, 1997.
11.Hautmann, S.H., Lokeshwar, V.B., Schroeder, G.L., Civantos, F., Duncan, R.C., Friedrich, M.G., Soloway, M.S. Elevated tissue expression of hyaluronic acid and hyaluronidase validate HA-HAase urine test for bladder cancer. J. Urol., 165: 2068-2074, 2000.
12. Setala, L.P., Tammi, M.I., Tammi, R.H., Eskelin, M.J., Lipponen, P.R., Argen, U.M., Parkkinen, J., Alhava, E.M., Kosma, V.M., Hyaluronan expression in gastric cancer cells is associated with local and nodal spread and reduced survival rate. Br. J. Cancer, 79: 1133-1138, 1999.
13. Auvinen, P., Tammi, R., Parkkinen, J., Tammi, M., Agren, U., Johansson, R., Hirvikoski, P., Eskelinen, M., Kosma, V.M., Hyaluronan in peritumoral stroma and malignant cells associates with breast cancer spreading and predicts survival. Am. J. Pathol., 156: 529-536, 2000.
14. Pirinen, R., Tammi, R., Tammi, M., Hirvikoski, P., Parkkinen, J.J., Johansson, R. Prognostic value of hyaluronan expression in non-small-lung cancer: increased stromal expression indicates unfavorable outcome in patients with adenocarcinoma. Int J Cancer 95: 12-27, 2001.
15. Knudson, W. Tumor associated hyaluronan: providing an extracellular matrix that facilitates invasion. Am. J. Pathol., 148: 1721-1726, 1996.
16. Ropponen, K., Tammi, M., Parkkinen, J., Eskelinen, M., Tammi, R., lipponen, P., Argen, V., Alhava, E., Kosma, V.M. Tumor-associated hyaluronan as an unfavorable prognostic factor in colorectal cancer. Cancer Res., 58:342-347, 1998.
17. Lipponen, P., Aaltomaa, S., Tammi, R., Tammi, M., Agren, U., Kosma, V.M. High stromal hyaluronan level is associated with poor differentiation and metastasis in prostate cancer. Eur. J. Cancer 37: 849-856, 2001.

18. Lokeshwar, V.B., Obek, C., Pham, H.T., Wei, D.C., Young, M.J., Duncan, R.C, Soloway, M.S., Block, N.L. Urinary hyaluronic acid and hyaluronidase: Markers for bladder cancer detection and evaluation of grade. J. Urol., 163: 348-356, 2000.
19. Lokeshwar, V.B., Obek, C., Soloway, M.S., Block, N.L. Tumor-associated hyaluronic acid: A new sensitive and specific urine marker for bladder cancer. Cancer Res., 57: 773-777, 1997.
20. Lokeshwar, V.B., Rubinowicz, D., Schroeder, G.L., Forgacs, E., Minna, J.D., Block, N.L. Nadji, M., Lokeshwar, B.L. Stromal and epithelial expression of tumor markers hyaluronic acid and hyaluronidase in prostate cancer. J. Biol. Chem. 276: 11922-11932, 2001.
21. Roden, L., Campbell, P., Fraser, J.R.E., Laurent, T.C., Petroff, H., Thompson, J.N. Enzymatic pathways of hyaluronan catabolism. In: The biology of hyaluronan. Whelan, E, (ed), Wiley, Chichister, Ciba Foundation Symp., 143, pp-60-86, 1989.
22. Csoka, A.B., Frost, G.I., Stern, R. The six hyaluronidase-like genes in the human and mouse genomes. Matrix Biol. 20: 499-508, 2001.
23.Lokeshwar, V.B., Lokeshwar, B.L., Pham, H.T., Block, N.L. Association of hyaluronidase, a matrix-degrading enzyme, with prostate cancer progression. Cancer Res., 56: 651-657, 1996.
24. Anderson, A.R., Feathergill, K., Diao, X., Cooper, M., Kirpatrick, R., Spear, P., Waller, D.P., Chany, C., Doncel, G.E., Herold, B., Zaneveld, L.J.D. Evaluation of poly(styrene-4-sulfonate) as a preventive agent for conception and sexually transmitted diseases. J. Androl., 21: 862-875, 2000.
25. Lokeshwar, V.B., Young M.J., Goudarzi, G., Iida, N., Yudin, A.I., Cherr, G.N., Selzer, M.G. Identification of bladder tumor-derived hyaluronidase: Its similarity to HYAL1. Cancer Res., 59: 4464-4470, 1999.
26. Sweat, S.D., Bergstralh, E.J., Slezak, J., Blute, M.L., Zincke, H. Competing risk analysis after radical prostatectomy for clinically nonmetastatic prostate adenocarcinoma according to clinical Gleason score and patient age. J Urol. 168: 525-529, 2002.
27. Lokeshwar, V.B., Öbek, C., Pham, H.T., Wei, D.C., Young, M.J., Duncan, R.C., Soloway, M.S., Block, N.L. Urinary hyaluronic acid and hyaluronidase: Markers for bladder cancer detection and evaluation of grade. J. Urol., 163: 348-356, 2000.
28. Lokeshwar BL, Selzer MG, Zhu BQ, Block NL, Golub LM. Inhibition of cell proliferation, invasion, tumor growth and metastasis by an oral non-antimicrobial tetracycline analog (COL-3) in a metastatic prostate cancer model. Int. J. Cancer 98: 297-309, 2002.
29. Church D, Zhang Y, Rago R. Efficacy of suramin against human prostate carcinoma DU145 xenografts in nude mice. Cancer Chemother Pharmacol. 43: 198-204, 1999.

THE JOURNAL OF BIOLOGICAL CHEMISTRY
Vol. 277, No. 37, Issue of September 13, pp. 33654–33663, 2002
Printed in U.S.A.

Regulation of Hyaluronidase Activity by Alternative mRNA Splicing*

Received for publication, April 19, 2002, and in revised form, June 3, 2002
Published, JBC Papers in Press, June 25, 2002, DOI 10.1074/jbc.M203821200

Vinata B. Lokeshwar‡§¶‖, Grethchen L. Schroeder‡, Robert I. Carey‡, Mark S. Soloway‡, and Naoko Iida‡¶

From the Departments of ‡Urology and §Cell Biology and Anatomy, University of Miami School of Medicine, Miami, Florida 33101

Hyaluronidase is a hyaluronic acid-degrading endoglycosidase that is present in many toxins and the levels of which are elevated in cancer. Increased concentration of HYAL1-type hyaluronidase correlates with tumor progression and is a marker for grade (G) 2 or 3 bladder cancer. Using bladder tissues and cells, prostate cancer cells, and kidney tissues and performing reverse transcription-PCR, cDNA cloning, DNA sequencing, and *in vitro* translation, we identified splice variants of HYAL1 and HYAL3. HYAL1v1 variant lacks a 30-amino acid (aa) sequence (301–330) present in HYAL1 protein. HYAL1v1, HYAL1v2 (aa 183–435 present in HYAL1 wild type), HYAL1v3 (aa 1–207), HYAL1v4 (aa 260–435), and HYAL1v5 (aa 340–435) are enzymatically inactive and are expressed in normal tissues/cells and G1 bladder tumor tissues. However, HYAL1 wild type is expressed in G2/G3 tumors and in invasive tumor cells. Stable transfection and HYAL1v1-specific antibody confirmed that the HYAL1 sequence from aa 301 to 330 is critical for hyaluronidase activity. All tumor cells and tissues mainly express HYAL3 variants. HYAL3v1 lacks a 30-aa sequence (299–328) present in HYAL3 protein, that is homologous to the 30-aa HYAL1 sequence. HYAL3v1, HYAL3v2 (aa 251–417 present in HYAL3 wild type), and HYAL3v3 (aa 251–417, but lacking aa 299–328), are enzymatically inactive. Although splicing of a single independent exon generates HYAL1v1 and HYAL3v1, internal exon splicing generates the other HYAL1/HYAL3 variants. These results demonstrate that alternative mRNA splicing controls cellular expression of enzymatically active hyaluronidase and may explain the elevated hyaluronidase levels in bladder/prostate cancer.

Hyaluronidases (HAases)[1] are a family of enzymes that are crucial for the spread of bacterial infections, toxins present in various venoms, and possibly, cancer progression (1–6). In humans, six HAase genes have been identified. These genes occur in clusters of three at two chromosomal locations (Ref. 7 and human genome blast search). HYAL1, HYAL2, and HYAL3 occur on chromosome 3p21.3, and PH20, HYAL4, and HYALP1 occur on chromosome 7q31.3. With the possible exception of HYAL4 and HYALP1, all other HAases degrade hyaluronic acid (HA) (7).

HA is a nonsulfated glycosaminoglycan made up of repeating disaccharide units, D-glucuronic acid, and *N*-acetyl-D-glucosamine. HA is present in body fluids, tissues, and the extracellular matrix (8–10). It keeps tissues hydrated and maintains osmotic balance and cartilage integrity (8, 10). HA also actively regulates cell adhesion, migration, and proliferation by interacting with specific cell surface receptors such as CD44 and RHAMM (11). The concentrations of HA are elevated in several inflammatory diseases and various carcinomas (*e.g.* bladder, prostate, breast, lung, colon, and so forth; Refs. 9 and 12–19). For example, we have shown that urinary HA concentration is a highly sensitive and specific marker for detecting bladder cancer, regardless of its grade (18, 19). In tumor tissues, HA may promote tumor growth and metastasis probably by actively supporting tumor cell migration and offering protection against immune surveillance (20–22). Small fragments of HA, generated by HAases, stimulate angiogenesis (23–25). We recently showed that HA fragments of ~10–15 disaccharide units stimulate endothelial cell proliferation by acting through cell surface HA receptor, RHAMM, and activating the mitogen-activated protein kinase pathway (26). We have also shown that elevated levels of HYAL1-type HAase coincide with the presence of angiogenic HA fragments in prostate tumor tissues and in the urine of bladder cancer patients (17, 27).

Among the six HAases, HYAL1, HYAL2, and PH20 are well characterized. HYAL1 type HAase was originally purified from human plasma and urine (28, 29). However, we have shown that HYAL1 is the major tumor-derived HAase expressed in bladder and prostate cancer tissues (17, 30). It has a optimum pH range of 4.0–4.3, and the enzyme is 50–80% active at pH 4.5 (17). Triggs-Raine *et al.* (31) have shown that a lack of functional HYAL1 results in a disorder called mucopolysaccharidosis IX. In this study the authors identified that aa Glu^{268} is crucial for HYAL1 activity. HYAL2 was originally designated as the lysosomal HAase, and it cleaves high molecular mass HA into ~20-kDa HA fragments (32). It has a pH optimum of ~4.0 and is possibly less active than other HAases. HYAL-2 may also be exposed to the cell surface through a GPI anchor (32). The third HAase gene in the 3p21.3 locus is HYAL3. Although

* This work was supported by National Institutes of Health Grant CA72821 (to V. B. L.), Department of Defense Grant DAMD 170210005 (to V. B. L.), and funds from the Sylvester Cancer Center. The costs of publication of this article were defrayed in part by the payment of page charges. This article must therefore be hereby marked "*advertisement*" in accordance with 18 U.S.C. Section 1734 solely to indicate this fact.

The nucleotide sequence(s) reported in this paper has been submitted to the GenBank™/EBI Data Bank with accession number(s)AF502904 (HYAL1v1), AF502905 (HYAL1v2), AF502906 (HYAL1v3), AF502907 (HYAL1v4), AF502908 (HYAL1v5), AF502909 (HYAL3v1), AF502910 (HYAL3v2), AF502911 (HYAL3v3), and AF502912 (HYAL3wt).

¶ Contributed equally to this work.

‖ To whom correspondence should be addressed: Dept. of Urology (M-800), University of Miami School of Medicine, P.O. Box 016960, Miami, FL 33101. Tel.: 305-243-6321; Fax: 305-243-6893; E-mail: vlokeshw@med.miami.edu.

[1] The abbreviations used are: HAase, hyaluronidase; aa, amino acid(s); HA, hyaluronic acid; NED, no evidence of disease; BT, bladder tumor; RT, reverse transcription; ELISA, enzyme-linked immunosorbent assay; TIM, triose phosphate isomerase.

HYAL3 transcripts have been detected in brain and liver tissues, its protein product is uncharacterized (31). Based on the sequence information deposited in GenBank™ HYAL3 is predicted to be made up of either 463 aa (accession number AF040710 (gi number 2935327)) or 417 aa (accession number BC012892 (gi number 15277616)).

Besides acidic HAases, PH20 (*i.e.* testicular HAase) is well characterized. PH20 is a sperm surface HAase that has a broad pH activity profile (pH 3.2–9.0) (33). In addition to being a HA-degrading enzyme, PH20 may also interact with HA to increase internal calcium, possibly by binding HA through aa 205–235 (34). This study also revealed that *N*-glycosylation and intrachain disulfide linkages are important for the HAase activity of PH20 (34).

Recently, the crystal structure of the bee venom HAase has been documented (35). The bee HAase shares ~30% sequence identity with human HAases. The crystal structure of bee HAase reveals a classical TIM barrel topology, where the catalytic site corresponds to Asp^{143} and Glu^{145} (aa numbering according to GenBank™ accession number AAA27730.1). Glu^{145} is involved the cleavage of the β-1,4 glycosidic bond between *N*-acetyl-D-glucosamine and D-glucuronic acid through an acid-base catalytic mechanism. These Asp and Glu residues are conserved in all mammalian HAases (32). For example, in HYAL1, the putative catalytic site residues are Asp^{131} and Glu^{133}, respectively, and in HYAL3, they are Asp^{127} and Glu^{129}, respectively (according to GenBank™ accession numbers AAD09137.2 and AAH12892.1). Based on the amino acid homology between bee HAase and mammalian HAases and conservation of several aa residues involved in both HA binding (*i.e.* substrate binding groove) and its catalysis (*i.e.* active site), a TIM barrel topology and a similar mechanism for the catalytic cleavage of HA are likely for the mammalian HAases (32).

In this study, we have identified several mRNA splice variants of HYAL1 and HYAL3 expressed in bladder and prostate cancer cells and in bladder and kidney tissues. These splice variants were characterized in terms of their protein product and HAase activity. We also identified a 30-aa region that is crucial for the HAase activity of HYAL1 and HYAL3 proteins.

EXPERIMENTAL PROCEDURES

Tissue Specimens—Normal bladder specimens were obtained from organ donors (20–50 years old), and the urothelial layer from these specimens was flash frozen after separation from the underlying muscle. Bladder tumor tissues (~1 g), bladder specimens with no evidence of disease (NED), and specimens of involved lymph node (*i.e.* local extension of tumor into lymph node) were obtained from bladder cancer patients undergoing cystectomy or transurethral resection of bladder tumor. The tissue specimens were split, and the mirror segment was examined by histology following fixation in formalin. In this study, we have included data from only those specimens that were histologically confirmed as normal and tumor (with grade information). All of the tissues were flash frozen and stored at −70 °C until use.

Tissue Culture—Established bladder cancer cell lines (*i.e.* HT1376, RT4, and UMUC-3) and prostate cancer cell lines (*i.e.* DU145 and LNCaP) were obtained from the American Type Culture Collection. Dr. Mark E. Stearns (Medical College of Pennsylvania, Philadelphia, PA) kindly provided the prostate cancer line PC3-ML (36). Bladder cancer cell lines 253J-Lung and 253J-parent were gifts from Dr. Colin Dinney (M. D. Anderson Cancer Center, University of Texas, Houston, TX) (37). All of these cell lines were cultured in RPMI 1640, 10% fetal bovine serum, and gentamicin. Primary normal bladder cell cultures were set up from the normal urothelium. The urothelial cells were gently scrapped from the bladder urothelium in RPMI 1640 containing 40% fetal bovine serum. The cell suspension (2 ml) was added to T-25 tissue culture flasks, and the cells were allowed to attach overnight. The following day, the nonadherent cells were washed off, and the cells were cultured in keratinocyte growth medium (Clonetics/BioWhitaker, San Diego, CA) until 80% confluence. The epithelial growth was confirmed by cytokeratin staining. Total RNA was extracted from the urothelial cultures on either the first or the second passage.

RT-PCR, cDNA Cloning, and Sequence Analyses—Total RNA was extracted from bladder/prostate cells, bladder tissues, and lymph node specimens using a RNA extraction kit (Qiagen). Total RNA from kidney tissues was purchased from BD Biosciences/CLONTECH (Palo Alto, CA). Total RNA (~1 μg) was subjected to first strand cDNA synthesis using a Superscript™ preamplification system and oligo(dT) primers (Invitrogen). The entire HYAL1 coding sequence was amplified from the first strand cDNA using a HYAL1-L3/HYAL1-R2 primer pair that we have used previously (17). HYAL1-L3 primer sequence is as follows: 5′-CTTCCTCCAGGAGTCTCTGGT-3′. The HYAL1-R2 primer sequence is as follows: 5′-ATCACCACATGCTCTTCCGC-3′. This primer pair should amplify a 1926-bp HYAL1 cDNA that contains the entire coding region of HYAL1 (618–1925). When compared with the HYAL1 clone HSU03056 that is deposited in GenBank™, HYAL1 cDNA amplified by the HYAL1-L3/HYAL1-R2 primer pair will contain an extra C at the 5′ terminus. This C is present in the human LUCA13 cosmid clone from the chromosome region 3p21.3 (GenBank™ accession number ACC002425). Thus, in this study, as compared with the HYAL1 clone HSU03056, the numbering of nucleotides in HYAL1wt and HYAL1 variant cDNAs is offset by 1.

To amplify HYAL3 cDNA, we used the following primer pair: 1) HYAL3-L2: The sequence of this primer corresponds to nucleotides 157–176 in the HYAL3 clone AF040710. This sequence is not present in the HYAL3 clone BC012892. HYAL3-L2 primer sequence is as follows: 5′-CCAGAGGCCAGCATCAACAT-3′. 2) HYAL3-R2: The sequence of this primer (5′-GACTCACATGATCTCAGAGG-3′) is reverse complementary to the sequence between nucleotides 1629 and 1648 in the HYAL3 clone AF502912, nucleotides 1628 and 1647 in the clone AF040710, and nucleotides between 1464 and 1483 in the clone BC012892. The HYAL3-L2/HYAL3-R2 primer pair should amplify a 1491-bp HYAL3 product. The amplification of HYAL1 and HYAL3 cDNAs was carried out by PCR as described previously (17). PCR products were analyzed by agarose gel electrophoresis and ethidium bromide staining.

The PCR products were directly cloned into the eukaryotic expression vector pcDNA3.1/v5/His-TOPO using a TOPO cloning kit (Invitrogen). This expression vector contains a strong cytomegalovirus promoter for eukaryotic expression, a neomycin resistance gene for selecting stable mammalian cell transfectants, and an ampicillin resistance gene for bacterial selection. All of the cloned HYAL1 and HYAL3 cDNAs were sequenced in an automated DNA sequencer in the DNA core facility at the University of Miami.

Generation of RT4 Stable Transfectants—RT4 cells (2×10^5 cells/6-cm dish) were transfected with 5 μg of either HYAL1 wild type (HYAL1wt) or HYAL1v1 (one of the HYAL1 variants) or pcDNA3.1/v5/His-TOPO vector using the Effectene™ transfection agent (Qiagen). Following 48 h of incubation in the growth medium (RPMI 1640, 10% fetal bovine serum, gentamicin), the transfectants were selected in neomycin (100 μg/ml)-containing growth medium. The RT4 clones resistant to neomycin were expanded and tested for HAase activity and HYAL1 protein expression using an HAase activity ELISA-like assay and immunoblot analysis, respectively, as described below.

In Vitro Translation—HYAL1 and HYAL3 cDNAs were *in vitro* translated using the TNT® Quick coupled transcription/translation system (Promega, Madison, WI). For generating [^{35}S]methionine-labeled product, 1 μg of cDNA (vector, HYAL1, or HYAL3) was mixed with TNT® Quick master mix and 20 μCi of Amersham Biosciences Redivue™ L-[^{35}S]methionine. The reaction was carried out at 30 °C for 90 min. Following incubation, 5-μl aliquots of each sample were mixed with 20 μg of bovine serum albumin and precipitated with equal volume of ice-cold 20% tricholoroacetic acid. The precipitates were centrifuged, washed twice in 10% tricholoroacetic acid, and washed once with 80% ice-cold ethanol. The precipitates were dissolved in SDS sample buffer and analyzed by 12% SDS-PAGE under reducing/nonreducing conditions.

Alternatively, the HYAL1/HYAL3 cDNAs or vector DNA were mixed with TNT® Quick master mix and 20 μM unlabeled L-methionine. The reaction was carried out at 30 °C for 90 min. The unlabeled *in vitro* translated products were analyzed for HAase activity by the ELISA-like assay.

HAase ELISA-like Assay—HAase ELISA-like assay has been described previously (17, 18, 38, 39). To assess HAase activity secreted by RT4 transfectants and bladder cancer cells, at ~60% confluence, various cultures were washed three times in phosphate-buffered saline and incubated in RPMI 1640 containing insulin, transferrin, and selenium solution (ITS supplement, Sigma-Aldrich). Following a 48-h incubation, the serum-free conditioned media were collected. For the HAase activity ELISA-like assay, various aliquots (0.5, 1.0, 2.5, 5.0, 7.5, and 10 μl)

of either *in vitro* translated samples, serum-free culture-conditioned media of different cells/transfectants or urine from bladder cancer patients or normal individuals were incubated with 96-well HA-coated microtiter plates in the presence of HAase assay buffer. Following incubation, the degraded HA was washed off, and the HA remaining on the wells was detected using a biotinylated HA-binding protein and an avidin-biotin detection system. The HAase present in each sample was calculated using a standard graph, which was prepared by plotting $A_{405\,nm}$ *versus* HAase concentration (units × 10^{-4}/ml) (18, 39). In the *in vitro* translated samples, the $A_{405\,nm}$ of each HYAL1/HYAL3 sample was subtracted from the $A_{405\,nm}$ of the vector sample, and the difference was used to determine the HAase activity.

Generation of Anti-HYAL1v1 Peptide Antibody—A 13-aa HYAL1v1 peptide (NH_2-TNHFLPLESCQAI-COOH) was synthesized, conjugated to keyhole limpet hemocyanin, and injected in New Zealand rabbits. The anti-HYAL1v1 antibody was purified using the HYAL1v1 peptide-conjugated affinity chromatography. The synthesis of HYAL1v1 peptide, generation of rabbit polyclonal antibody, and affinity purification were carried out by ResGen™ Invitrogen Corp. (Huntsville, AL).

Immunoblot Analysis—Conditioned media of bladder cancer cells and stable transfectants and urine specimens were separated by 8.5% SDS-PAGE under nonreducing conditions. The gels were blotted on to polyvinylidene difluoride membranes. The blots were probed with either anti-HYAL1 peptide IgG (30) or anti-HYAL1v1peptide affinity-purified IgG at 4 °C for 16 h. The blots were developed using an alkaline phosphatase detection system, as described previously (30).

RESULTS

Detection of HYAL1 Splice Variants by RT-PCR, cDNA Cloning, and Sequence Analysis—Based on the Human Genome Blast search, HYAL1 gene contains three exons separated by two introns (NT_006014.7/HS3_6171, *Homo sapiens* chromosome 3 working sequence). It has been previously shown that the untranslated region in exon 1 between nucleotides 110 and 596 is alternatively spliced (GenBank™ accession number AF173154). To detect the expression of HYAL1 in various cancer cells, tumor tissues, and normal kidney tissue, we performed RT-PCR analysis using a HYAL1-specific primer pair. This primer pair should amplify the entire HYAL1 coding region (bp 618–1926), an untranslated region in exon 1 that is alternatively spliced (nucleotide 110 joining 596), and the first 110 bp. Thus, the length of the expected PCR product is 1926 nucleotides. Fig. 1 (*A* and *B*) shows two gels in which PCR products from various samples were analyzed. The different tissue specimens are numbered (*e.g.* NBL-1 to NBL-4; G1-BT-1 to G1-BT-3; G2-BT-1 and G2-BT-2; G3-BT-1 to G3-BT-3; NED1-1; NED-2; LN-1 and LN-2). An approximately 1.4-kb product is amplified from bladder cancer cells (*i.e.* HT1376, 253J-Lung, 253J-parent, and UMUC-3), prostate cancer cells (*i.e.* DU145, LNCaP, and PC3-ML), G2 and G3 bladder tumor tissues (G3-BT-1, G2-BT-1, G2-BT-2, G3-BT-2, and G3-BT-3), lymph node specimens invaded with bladder tumor (LN-1 and LN-2) and normal kidney tissue (Fig. 1, *A* and *B*). RT4 RNA sample showed negligible amplification of any HYAL1-related PCR products. A smaller ~1.3-kb PCR product is also amplified from 253J-Lung and HT1376 RNA samples (Fig. 1*A*). The same ~1.3-kb PCR product was also detected in the kidney tissue and some bladder tumor tissue specimens when electrophoresis was carried out for a longer period of time to allow separation between ~1.4- and ~1.3-kb PCR products (data not shown). As shown in Fig. 1 (*A* and *B*), an approximately 500-bp PCR product is amplified from RNA samples isolated from a primary normal bladder cell culture (NBL cells), normal bladder tissues (NBL-1, NBL-2, NBL-3, and NBL-4), kidney tissue, and G1 bladder tumor tissues (G1-BT-2 and G1-BT-3). An approximately 650-bp PCR product is also amplified from two G1 bladder tumor tissues (G1-BT-1 and G1-BT-3), NBL2 tissue, normal kidney tissue, and an LN-2 specimen (Fig. 1, *A* and *B*). An approximately 1.0-kb PCR product is amplified from a G3 bladder tumor tissue (G3-BT-1) and an LN-1 specimen (Fig. 1 A and B). A slightly larger PCR product (~1.1-kb) was detectable in NBL-4 and kidney tissue samples (Fig. 1*B*).

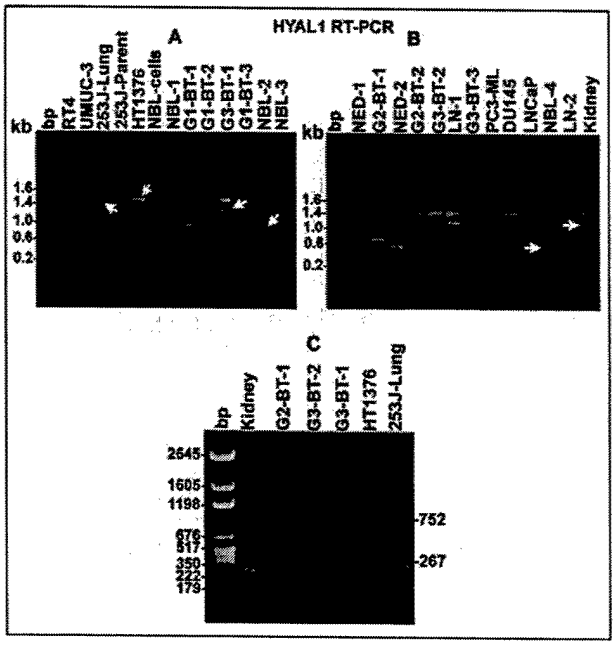

FIG. 1. **Examination of HYAL1 expression in tissues and cells.** Total RNA extracted from bladder tissues, bladder cells (tumor cells: RT4, UMUC-3, 253J-Lung, and 253J-parent and HT1376; NBL cells: normal bladder cells), prostate cancer cells (PC3-ML, DU145, and LNCaP) was subjected to RT-PCR analysis using HYAL1-specific primers as described under "Experimental Procedures." The PCR products were analyzed by agarose gel electrophoresis. Six PCR products of different lengths are marked. PCR products expressed in each of these tissues or cells were cloned and sequenced. The tissue specimens in each category are numbered (*e.g.* NBL-1, NBL-2, G1-BT-1, G3-BT-1, LN-1, etc.). *A* and *B*, RT-PCR analysis using primer pair HYAL1-L3 and HYAL1-R2. This primer pair should amplify an approximately 1.9-kb HYAL cDNA (*i.e.* 1–1926 bp) that contains the HYAL1 coding region (618–1925 bases). A 200-bp ladder (Promega) was used a bp marker. *C*, RT-PCR analysis using the primer pair HYAL1-L3 and HYAL1-R3. This primer pair should amplify a 267- or 752-bp PCR product depending upon the splicing status of the HYAL1 transcript related to the untranslated region between nucleotides 110–596. pGEM markers (Promega) were used as a bp ladder.

Because the RT-PCR analysis described above does not result in the amplification of an approximately 1.9-kb PCR product that is expected based on the primer pair design, there could be two possibilities. First, such a product may have been missed because of the large size of the PCR product, and second, bladder tissues/cells contain only the HYAL1 transcript in which the bp between 110 and 596 are spliced out. The second possibility is based on the sequences deposited in GenBank™, which show that the 5′-untranslated region between nucleotides 110 and 596 is alternatively spliced (*e.g.* accession numbers HSU03056 and AF173154). To test these possibilities we performed RT-PCR analysis using a HYAL1 primer pair (*i.e.* HYAL1-L3/HYAL1-R3) that lies outside the boundaries of the spliced region. This primer pair would generate a 267-bp PCR product if the region between nucleotides 110 and 596 is spliced out, and a 752-bp PCR product will be generated if the HYAL1 transcript is unspliced. We have previously used this primer pair to demonstrate the presence of HYAL1 splicing in this region in prostate cancer cells (17). As shown in Fig. 1*C*, a major 267-bp PCR-amplified product is present in all samples, which include kidney, G2-BT-1, G3-BT-2, G3-BT-1, HT1376, and 253J-Lung. However, a minor 752-bp product is visible in bladder cancer cells and bladder tumor tissues. The presence and absence of the region between nucleotides 110 and 596 was

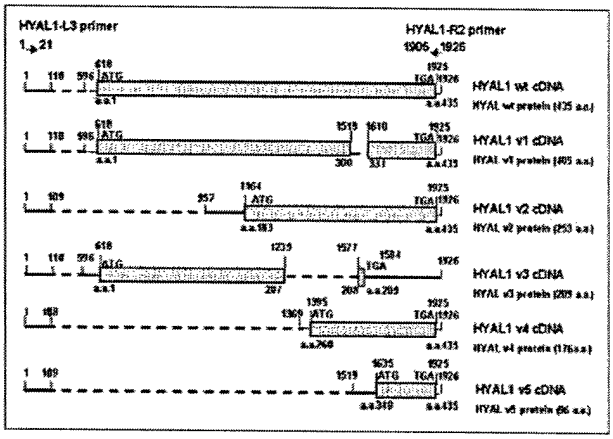

FIG. 2. **A schematic representation of the HYAL1 splice variants.** The figure shows HYAL1wt and different splice variant cDNAs. The numbering is based on the sequence of cDNA clone HSU03056 that is deposited in GenBank™. However, the numbering is offset by 1. This is because HSU03056 clone lacks the nucleotide C that is present in the 5′ terminus of all HYAL1 clones described in this study. The coding region is shown as a *dotted block*. The *dashed line* shows the region that is spliced out, and *solid line* represents untranslated regions. Each splice junction is marked by the nucleotides at the 5′ and 3′ boundaries that are joined because of splicing. The translation initiation and termination codons for HYAL1wt and HYAL1 variants are marked. The figure also shows the position of the forward (*i.e.* HYAL1-L3) and the reverse complementary (*i.e.* HYAL1-R2) primer pair used to amplify HYAL1 cDNA. The sequences of these primers are given under "Experimental Procedures."

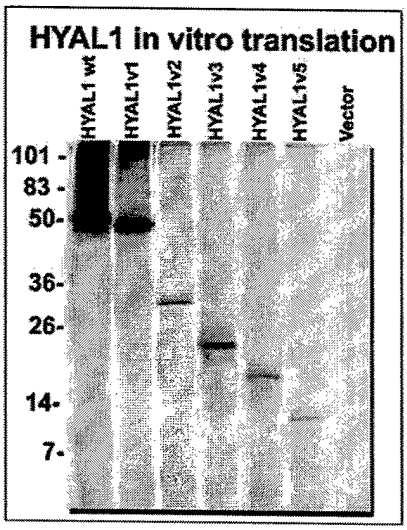

FIG. 3. ***In vitro* transcription/translation of HYAL1wt and HYAL1 variant cDNAs.** Various HYAL1 cDNAs and plasmid vector DNA were transcribed and translated *in vitro* using a coupled transcription/translation system and ^{35}S-labeled methionine, as described under "Experimental Procedures." The ^{35}S-labeled proteins were analyzed by SDS-PAGE along with molecular mass markers as described under "Experimental Procedures."

confirmed by cDNA cloning and sequencing of the 267- and 752-bp PCR products as we described before (17). These results indicate that it is very likely that the HYAL1 transcripts in which the region between nucleotides 110 and 596 is unspliced are not the major HYAL1 transcripts expressed in bladder tumor tissues and cells. Furthermore, lack of amplification of an approximately 1.9-kb PCR product in tissue/cell specimens may be due to some technical difficulty associated with the amplification of large PCR products.

All of the different PCR products from each sample were gel-isolated and directly cloned into the eukaryotic expression vector pcDNA3.1/v5/His-TOPO. The sequence analyses revealed that various PCR products represent HYAL1 mRNA splice variants. The cDNA and amino acid sequences of each of the five HYAL1 splice variants described in this study have been deposited in GenBank™. As shown in Fig. 2, the ~1.4-kb product is actually 1441 bases in length and is generated by splicing of the region from nucleotides 109 to 595 and, thus, joining nucleotides 110–596. This HYAL1 splice variant that arises from an internal splicing event in exon 1 has been identified previously (GenBank™ accession number AF173154 (gi number 5825510)). For the purpose of this study, we have designated the 1441-bp HYAL1 cDNA as HYAL1wt. The cloned HYAL1wt cDNA encodes the intact wild type HYAL1 protein consisting of 435 aa, the sequence of which is identical to that deposited in GenBank™ (accession number AAD09137.2)

The actual length of the ~1.3-kb product is 1351 bases. It lacks the region in Exon 1 between nucleotides 110 and 596 and, in addition, contains a deletion that joins nucleotides 1519 and 1610 (*i.e.* nucleotides 1520–1609 are deleted; Fig. 2). This cDNA, designated as HYAL1v1 (HYAL1 variant 1; GenBank™ accession number AF502904), can encode a protein that is 405 aa in length. When compared with the HYAL1wt protein sequence, the HYAL1v1 protein lacks 30 aa from aa 301–330. Thus, in the putative HYAL1v1 protein, aa 300 is joined to aa 331 (Fig. 2).

The HYAL1v2 cDNA consists of 1084 bases (Fig. 2). In this variant, nucleotide 109 is joined to nucleotide 952, *i.e.* the sequence from nucleotides 110 to 951 is deleted (GenBank™ accession number AF502905). If the HYAL1v2 variant is translated, using an ATG at position 1164 as the start codon, it will generate a protein consisting of 253 aa. The sequence of the putative HYAL1v2 protein is identical to the HYAL1wt protein sequence from aa 183 to 435.

The slightly larger ~1.1-kb HYAL1 variant is designated as HYAL1v3, and it is 1104 bases in length (Fig. 2). HYAL1v3 contains two spliced regions; in the first, nucleotide 110 joins nucleotide 596, and in the second, nucleotide 1239 joins nucleotide 1577 (*i.e.* bases from 1240 to 1576 are deleted; GenBank™ accession number AF502906). If HYAL1v3 is translated, it will utilize ATG^{618} as the start codon and generate a protein consisting of 209 aa (Fig. 2). The first 207 aa of the putative HYAL1v3 protein are identical to the first 207 aa of the HYAL1wt protein.

The ~0.65-kb PCR product originates from a HYAL1v4 variant whose actual length is 666 bases (Fig. 2). The HYAL1v4 cDNA contains a deletion starting from nucleotide 109 and ending at nucleotide 1368. Thus, in the HYAL1v4 cDNA, nucleotide 108 is joined to nucleotide 1369 (GenBank™ accession number AF502907). The HYAL1v4 cDNA contains an open reading frame starting at ATG^{1395} that allows translation of a polypeptide consisting of 176 aa. The aa sequence of the putative HYAL1v4 protein is identical to the aa sequence of HYAL1wt starting with aa 260–435 (Fig. 2).

The splice variant HYAL1v5 consists of 517 bases, and this variant is generated by splicing of nucleotides 109 and 1519 (GenBank™ accession number AF502908). If ATG^{1635} is used as the start codon, the HYAL1v5 variant will encode a protein made up of 96 aa, the sequence of which is identical to the HYAL1wt protein sequence from aa 340 to 435 (Fig. 2).

In Vitro Translation and Analysis of HAase Activity of HYAL1 Variant Proteins—To determine whether various HYAL1 variants encode HAase activity, we used a coupled *in vitro* transcription/translation system and ^{35}S-labeled L-methionine to generate HYAL1wt and HYAL1 variant proteins. As shown in Fig. 3, the *in vitro* translated HYAL1wt and HYAL1 variant (v1–v5) proteins are of molecular mass ~50, ~47, ~30,

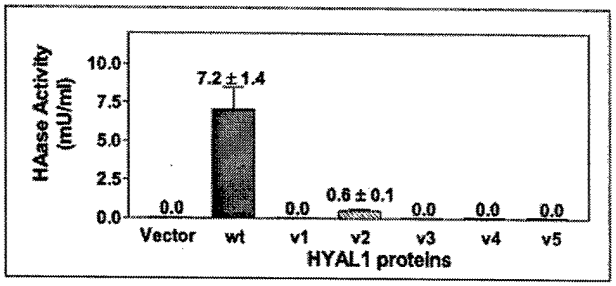

FIG. 4. **Analysis of HAase activity of HYAL1wt and HYAL1 variant proteins.** *In vitro* translated, unlabeled HYAL1wt and HYAL1 variant proteins, as well as vector-only control were analyzed for HAase activity using the HAase activity ELISA-like assay as described under "Experimental Procedures." Each sample was assayed at five different concentrations in duplicate. The results represent milliunits/ml ± S.E. Each experiment was repeated twice and independently.

~20, and ~10 kDa. The molecular mass of these proteins is similar to the expected molecular mass of the HYAL1wt and various HYAL1 variant polypeptides, based on their deduced aa sequences. The reduced intensities of the ^{35}S-labeled HYAL1v2, HYAL1v3, HYAL1v4, and HYAL1v5 proteins are most likely not due to reduced synthesis but to the reduced number of methionine residues present in these polypeptides. Based on the deduced aa sequence, HYAL1wt and HYAL1v1 proteins contain 9 methionines, whereas HYAL1v2, HYAL1v3, HYAL1v4, and HYAL1v5 proteins contain 6, 4, 4, and 3 methionines, respectively.

The HAase activity of *in vitro* translated HYAL1 variant proteins was measured using an ELISA-like assay (30, 39). Because we have previously shown that HYAL1 type HAase has a pH optimum at 4.2 (range 4.0–4.3; Ref. 30), the HAase ELISA-like assay was carried out at pH 4.2. As shown in Fig. 4, no HAase activity is detected in the vector only sample. However, the *in vitro* translated HYAL1wt protein has measurable HAase activity (7.2 ± 1.4 milliunits/ml). Interestingly, the HYAL1v1 protein that lacks only 30 aa (aa 301–330) has no HAase activity (Fig. 4). It is noteworthy that the HYAL1v1 protein contains both the putative HAase catalytic site (Asp^{131} and Glu^{133}) and Glu^{268}, which are critical for HAase activity of HYAL1 (Figs. 2 and 4 and Ref. 31). The HYAL1v2 protein that lacks the putative catalytic site but retains Glu^{268} and the 30-aa sequence shows less than 90% of HAase activity (0.6 ± 0.1 milliunits/ml) when compared with the HYAL1wt protein. No HAase activity is detected in HYAL1v3, HYAL1v4, and HYAL1v5 proteins. We also conducted the HAase ELISA-like assay at pH 3.7, 5.0, and 7.0, and none of the HYAL1 variants showed any activity at these pH levels (data not shown). These results demonstrate that although the catalytic site in HYAL1 may lie in the amino-terminal third of the protein, a 30-aa sequence from aa 301 to 330 is also critical for HAase activity.

Evaluation of HAase Expression in Stable Transfectants Expressing HYAL1wt and HYAL1v1 cDNA Constructs—It is possible that when translated *in vitro*, the HYAL1v1 protein does not fold correctly and/or lacks some post-translational modifications that are necessary for HAase activity. To test this possibility, we stably transfected RT4 bladder cancer cells with plasmid vector DNA, HYAL1wt, or HYAL1v1 cDNA constructs. We have previously shown that HYAL1 is not expressed in RT4 cells and that these cells do not secrete any HAase activity in their culture-conditioned media. We analyzed 10 stable clones of RT4 cells/construct (*i.e.* vector, HYAL1wt, and HYAL1v1) for HAase activity and HYAL1-related protein expression. The data on two representative clones/construct are shown in Figs. 5 and 6. Fig. 5*A* shows immunoblot analysis of culture-conditioned media of RT4 clones and HT1376 and 253J-lung cells using an anti-HYAL1 peptide IgG (30). The anti-HYAL1 peptide IgG was generated against a peptide sequence in HYAL1 between aa 321 and 338 (30). Thus, this antibody will be able to recognize HYAL1wt and variant proteins HYAL1v2 and HYAL1v4. However, it will not detect other variant proteins (*i.e.* HYAL1v1, HYAL1v3, and HYAL1v5) that either partially or completely lack this sequence. Although no expression of HYAL1-related protein is observed in the vector only clones, an approximately 60-kDa HYAL1 protein is detected in the conditioned media of HYAL1wt clones and HT1376 and 253J-lung cells. The molecular mass of the HYAL1wt protein detected in the conditioned media is higher than that generated by *in vitro* translation (~50 kDa), indicating that HYAL1 protein is glycosylated or modified by other post-translational modifications. It is noteworthy that the anti-HYAL1 peptide IgG was able to immunoprecipitate [^{35}S]methionine-labeled HYAL1wt polypeptide generated by *in vitro* translation (data not shown). The smaller product observed in the conditioned media of HT1376 and 253J-Lung cells is most likely a degradation product. This is because these cells do not express HYAL1 v2 and HYAL1v4 transcripts (as seen in Fig. 1A), and furthermore, the molecular mass of this product (~45 kDa) is larger than those of the expected HYAL1 v2 and HYAL1 v4 products.

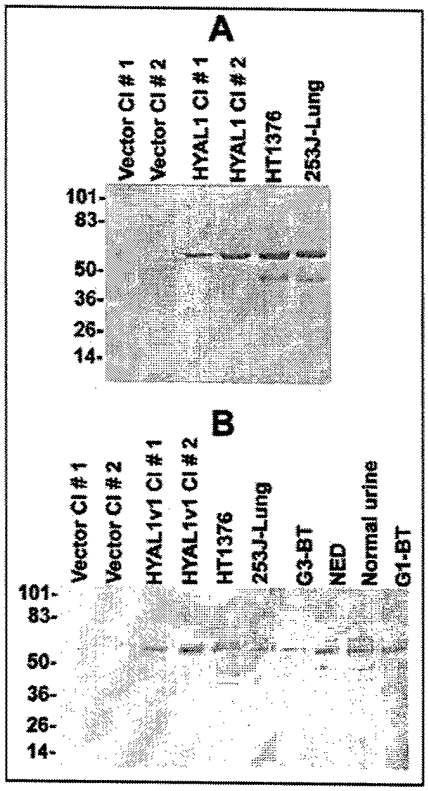

FIG. 5. **Immunoblot analysis of HYAL1 and HYAL1v1 expression.** Serum-free culture-conditioned media of RT4 stable transfectant (*i.e.* vector only, HYAL1wt, and HYAL1v1; two clones/construct), bladder cancer cells, and patient urine were subjected to either anti-HYAL1 or anti-HYAL1v1 peptide IgG immunoblot analysis as described under "Experimental Procedures." *A*, immunoblot analysis using anti-HYAL1 peptide IgG. *HYAL1* indicates HYAL1wt. *B*, immunoblot analysis using an affinity-purified anti-HYAL1v1 IgG. *G3-BT*, urine specimen obtained from a patient with G3 bladder tumor; *G1-BT*, urine specimen obtained from a patient with G1 bladder tumor; *NED*, urine specimen obtained from a patient with a history of bladder cancer but no disease at the time of specimen collection.

Fig. 5*B* shows immunoblot analysis of conditioned media of HYAL1 v1 transfectants of RT4, HT1376, and 253J-Lung cells

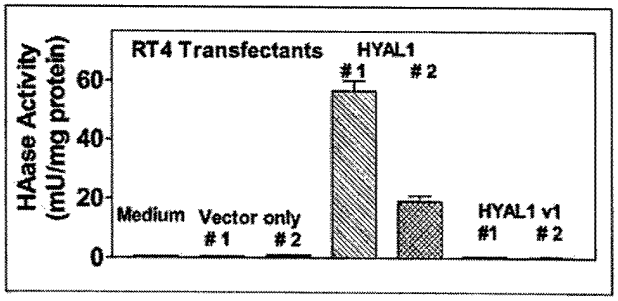

FIG. 6. **Analysis of HAase activity secreted by RT4 stable transfectants.** Serum-free culture-conditioned media of two clones each of vector only, HYAL1wt, and HYAL1v1 RT4 transfectants were assayed for HAase activity using the ELISA-like assay as described under "Experimental Procedures." Five concentrations of each sample were assayed in duplicate in each experiment, and each experiment was independently repeated three times. The HAase activity was normalized to total protein (mg/ml) and expressed as milliunits/mg protein ± S.E.

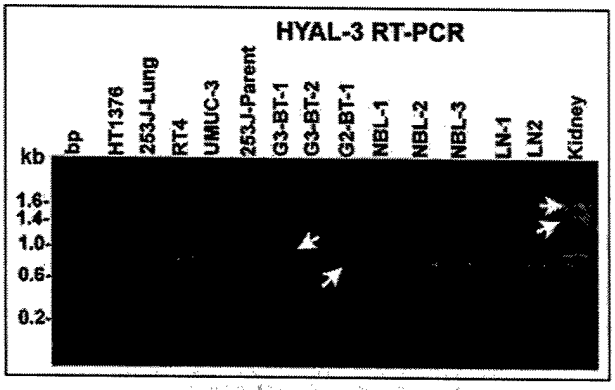

FIG. 7. **Examination of HYAL3 expression in tissues and cells.** Total RNA extracted from bladder tissues, bladder cells (RT4, UMUC-3, 253J-Lung, 253J-parent, and HT1376), and lymph node specimens invaded with bladder tumor was subjected to RT-PCR analysis using HYAL3 specific primers as described under "Experimental Procedures." The PCR products were analyzed by agarose gel electrophoresis. Four PCR products of different lengths are marked. PCR products expressed in each of these tissues or cells were cloned and sequenced. A 200-bp ladder (Promega) was used a bp marker.

and urine specimens using an anti-HYAL1v1 affinity-purified peptide IgG. The anti-HYAL1v1 antibody was generated against a 13-aa peptide in which the 300th aa present in the HYAL1 sequence is juxtaposed with 331st aa Such a peptide can occur only in the HYAL1v1 protein, in which the aa 300 is joined to aa 331 because of mRNA splicing. Therefore, this antibody is specific for HYAL1v1 and does not detect other HYAL1 proteins. As expected, no HYAL1v1 protein is detected in the conditioned media of vector only clones. However, an approximately 57-kDa protein is detected in the conditioned media of HYAL1v1 clones. Interestingly, the protein detected by anti-HYAL1v1 peptide IgG is also present in the conditioned media of HT1376 and 253J-Lung cells and in the urine of bladder cancer patients (G3-BT and G1-BT), a patient with bladder cancer history but no disease at the time of urine collection, and normal individual (Fig. 5*B*). The faint smaller bands that are observed in some samples are possibly degradation products that may be generated during sample storage. The fact that the molecular mass of the HYAL1v1 protein is larger than the HYAL1v1 polypeptide generated by *in vitro* translation suggests that the HYAL1v1 protein is also post-translationally modified. The secretion of both the cloned and naturally occurring HYAL1v1 protein in the culture-conditioned media suggests that the HYAL1v1 protein is folded and processed correctly. It should be noted that the ~57-kDa protein detected by anti-HYAL1v1 IgG in the immunoblot analysis is HYAL1v1, because the affinity-purified anti-HYAL1v1 IgG was able to immunoprecipitate HYAL1v1 polypeptide generated by *in vitro* translation (data not shown).

We next measured the HAase activity secreted in the conditioned media of various RT4 transfectants, and the activity was normalized to total protein in the conditioned media. As shown in Fig. 6, there is no detectable HAase activity in the medium control and in the conditioned media of the vector only clones. However, the two HYAL1wt clones secrete high levels of HAase activity (*i.e.* clone number 1: 56.5 ± 3.5 milliunits/mg protein and clone number 2: 27 ± 4 milliunits/mg protein). However, no HAase activity is detected in the conditioned media of RT4 clones that express and secrete HYAL1v1 protein. These results demonstrate that the HYAL1v1 protein is enzymatically inactive and that the sequence from aa 301 to 330 is critical for the activity of HYAL1 protein.

Detection of HYAL3 Splice Variants, cDNA Cloning, and Sequencing—Because the chromosomal locations are similar in HYAL1, HYAL2, and HYAL3 genes (7, 32, 40), we examined whether HYAL3 might also be similarly spliced and generate splice variants. The Human Genome Blast search reveals that HYAL3 gene contains four exons separated by three introns (NT_006014.7/HS3_6171, *H. sapiens* chromosome 3 working sequence). To HYAL3 expression, we performed RT-PCR analysis on RNA extracted from bladder cancer lines (*i.e.* HT1376, 253J-Lung, RT4, UMUC-3, and 253J-parent), bladder tissues (*i.e.* normal and tumor), lymph node positive for tumor, and normal kidney tissue. The primer pair that we used for PCR analysis was designed to amplify a full-length HYAL3 cDNA, 1.5-kb in length. As shown in Fig. 7, an approximately 1.5-kb product is amplified from normal kidney tissue RNA. A smaller ~1.4-kb product is also visible in the kidney tissue sample that is detectable in many bladder cancer cell lines. The major PCR amplification product that is present in all bladder cancer cells, tissues, and lymph node specimens is ~600 bp in length (Fig. 7). This product is also present in the kidney tissue sample, along with an approximately 700-bp product. In addition, the 700-bp product is amplified from RNA extracted from G3 bladder tumor tissue (*i.e.* G3-BT-1), normal bladder tissue (*i.e.* NBL-3), and normal kidney tissue.

The ~1.5, ~1.4, ~0.7, and 0.6-kb PCR products were gel-isolated and directly cloned into the eukaryotic expression vector pcDNA3.1/v5/His-TOPO. The sequence analyses revealed that different PCR products represent HYAL3 splice variants. As shown in Fig. 8, the ~1.5-kb splice variant is actually 1492 bases in length. The sequence of this cDNA is 100% homologous to the HYAL3 clone AF040710 from nucleotides 157 to 1647, except that our cDNA has an extra G at position 1422 (GenBank™ accession number AF502912). This G is present in other HYAL3 cDNA clones (*e.g.* BC012892) and in the cosmid clone LUCA14 from 3p21.3, sequences of which are deposited in GenBank™ (accession numbers gi16164953, gi15208650, gi13543476, and AF036035). The G at position 1422 is also present in all of the HYAL3 splice variants identified in this study. Because of the presence of this G, translation of the HYAL3 polypeptide terminates at position 1447 (TAA termination codon position 1445–1447) and generates a 417-aa protein (Fig. 8).

The ~1.4-kb PCR product contains 1402 bases. As shown in Fig. 8, this sequence contains a 90-base deletion that joins nucleotides 1089 and 1180 (*i.e.* nucleotides 1090–1179 are deleted). This cDNA is designated as HYAL3v1 and can encode a protein made up of 387 aa (GenBank™ accession number AF502909). The putative HYAL3v1 protein contains a 30-aa deletion that involves aa 299–328. Thus, in the HYAL3v1

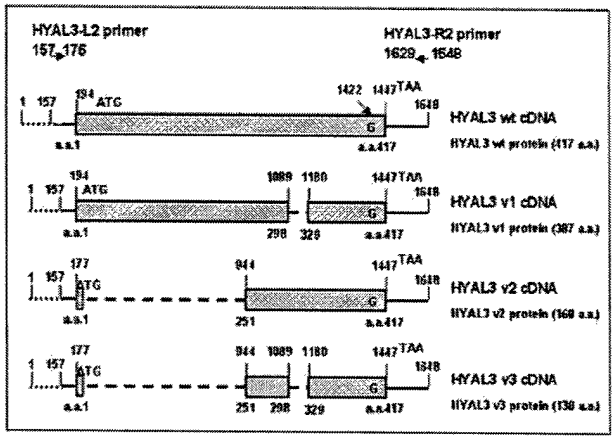

FIG. 8. **A schematic representation of the HYAL3 splice variants.** The figure shows HYAL3wt and different splice variant cDNAs. The numbering is based on the sequence of cDNA clone AF040710 that is deposited in GenBank™. However, the numbering is offset by 1 after nucleotide 1422. This is because the AF040710 is missing a G at position 1422. The coding region is shown as a *dotted block*. The *dashed line* shows the region that is spliced out, and the *solid line* represents untranslated regions. The *dotted line* between nucleotides 1 and 157 indicates the portion missing in our cDNAs. Each splice junction is marked by the nucleotides at the 5′ and 3′ boundaries that are joined because of splicing. The translation initiation and termination codons for HYAL1wt and HYAL1 variants are marked. The figure also shows the position of the forward (*i.e.* HYAL3-L2) and the reverse complementary (*i.e.* HYAL3-R2) primer pair used to amplify HYAL3 cDNA. The sequences of these primers are given under "Experimental Procedures," and the numbering is according to HYAL3 clone deposited in GenBank™ (accession number AF502912).

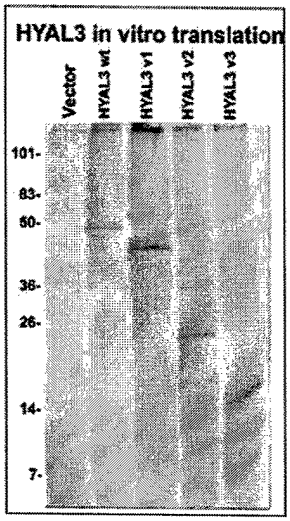

FIG. 9. ***In vitro* transcription/translation of HYAL3wt and HYAL3 variant cDNAs.** Various HYAL3 cDNAs and plasmid vector DNA were transcribed and translated *in vitro* using a coupled transcription/translation system and ^{35}S-labeled methionine, as described under "Experimental Procedures." The ^{35}S-labeled proteins were analyzed by SDS-PAGE along with molecular mass markers as described in "Experimental Procedures."

protein, aa 298 is joined to aa 329. The ~0.7-kb HYAL3 PCR product is actually 726 bases in length. The sequence analysis reveals that this variant (designated as HYAL3v2) is generated by a 766-base deletion that joins nucleotides 177 and 944 (Fig. 8; GenBank™ accession number AF502910). The HYAL3v2 variant would encode a 168-aa polypeptide in which aa 2–168 are identical to aa 251–417 in HYAL3wt protein. The smallest HYAL3 variant, HYAL3v3, is 636 bases in length. It is generated by two splicing events; in the first event, nucleotides 177 and 944 join, and in the second, the 90 bases between nucleotides 1089 and 1180 are deleted (as observed in HYAL3v1, Fig. 8; GenBank™ accession number AF502911). As shown in Fig. 8, the HYAL3v3 cDNA would encode a 138-aa protein, which like the HYAL3v2 protein is 100% homologous to aa 251–417 in the HYAL3wt sequence, except that it lacks the 30 aa sequence from aa 299 to 328.

In Vitro Translation and Examination of HAase Activity of HYAL3wt and Variant Proteins—Various HYAL3 cDNAs were *in vitro* translated using the coupled transcription/translation system and ^{35}S-lableled methionine. As shown in Fig. 9, HYAL3wt, HYAL3v1, HYAL3v2, and HYAL3v3 cDNAs upon *in vitro* transcription and translation generate polypeptide chains with molecular masses ~48, ~45, ~20, and ~16 kDa, respectively. The molecular masses of these proteins are comparable with the expected molecular masses based on the number of aa present in HYAL3wt and variant polypeptide chains. No protein is detected with vector only (Fig. 9, *Vector*).

We next measured the HAase activity of *in vitro* translated HAYL3 proteins. Because the HYAL3 gene is located in the same chromosomal location as the HYAL1 and HYAL2 genes, we assumed that like the HYAL1 and HYAL2 proteins, the HYAL3 protein may also have an acidic pH optimum (32). Therefore, we assayed the HAase activity of *in vitro* translated HAYL3 proteins at pH 4.2, using the HAase activity ELSA-like assay (17). As shown in Fig. 10, no HAase activity is detected with vector only. However, HYAL3wt protein has measurable HAase activity (7.4 ± 1.4 milliunits/ml). The HYAL3v1 variant that lacks the 30-aa sequence from aa 299 to 328 but retains the putative enzyme catalytic site (Asp^{127} and Glu^{129}; Ref. 32) and Glu^{266}, which may also be important for HAase activity (31), has no HAase activity (Fig. 10). The HYAL3v2 variant that retains the 30-aa sequence and Glu^{266} but lacks the putative enzyme catalytic site is also enzymatically inactive (Fig. 10). The HYAL3v3 variant that contains only Glu^{266} and lacks both the putative enzyme catalytic site and the 30-aa sequence has no HAase activity. These results demonstrate that in addition to the putative catalytic site and possibly Glu^{266}, the 30-aa sequence from aa 299 to 328 is critical for HAase activity of the HYAL3 protein.

Comparison of the 30-aa Sequence between HYAL1, HYAL3, and Other HAases—Because in both HYAL1 and HYAL3 proteins a 30-aa sequence appears to be critical for HAase activity, we compared this sequence present in both proteins. As shown in Fig. 11, the 30-aa sequence present in HYAL1 (aa 301–330) and HYAL3 (aa 299–328) appears to be similarly situated in both proteins. In this 30-aa sequence, 17 aa among the first 22 are either identical or conserved substitutions. When a comparable 30-aa sequence among other human HAases (*i.e.* HYAL2, HYAL4, and PH20) is aligned, 17 of the first 22 aa are highly conserved (*i.e.* identical or conserved substitutions). Furthermore, the conserved aa occur at positions 2, 3, 6–8, 10–12, and 14–22. In addition, at position 29, either a Ser or a Thr residue is present in all HAases. In HYALP1, which is possibly a pseudogene (7), the 30-aa region also appears to be conserved, and of the first 22 aa in this sequence, 16 are conserved. In HYALP1, a Ser residue is present at position 29. We also compared a similarly positioned 30-aa sequence in bee HAase. As shown in Fig. 11, of the first 22, 12 are conserved (either identical or conserved substitutions) that occur at positions 2, 3, 6, 7 14, 15, and 17–22. In addition, Thr at position 29 is also conserved. The high sequence homology among mammalian and invertebrate HAases with respect to the 30-aa sequence suggests that this sequence is critical for HAase structure and activity.

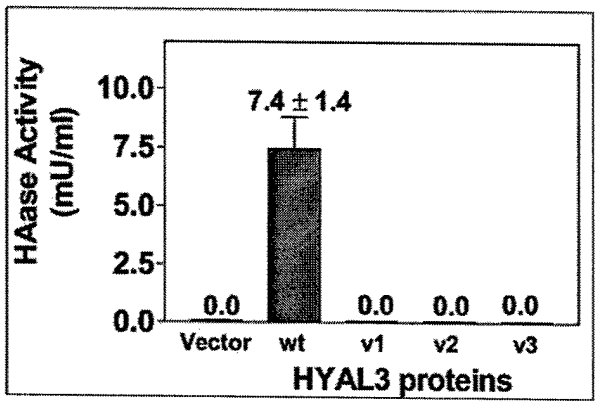

FIG. 10. **Analysis of HAase activity of HYAL3wt and HYAL3 variant proteins.** *In vitro* translated, unlabeled HYAL3wt and HYAL3 variant proteins, as well as vector-only control were analyzed for HAase activity using the HAase activity ELISA-like assay as described under "Experimental Procedures." Each sample was assayed at five different concentrations in duplicate. The results represent milliunits/ml ± S.E. Each experiment was repeated twice and independently.

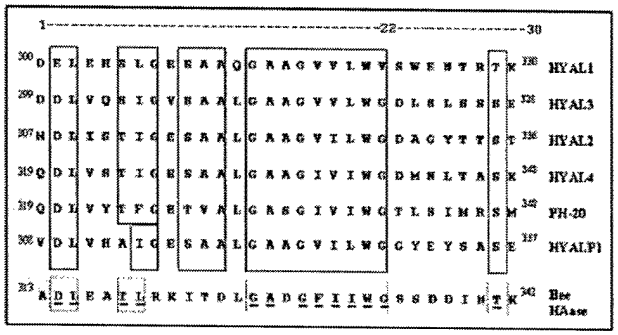

FIG. 11. **Comparison of a 30-aa sequence in various human and bee HAases.** The 30-aa sequences identified in HYAL1 and HYAL3 type HAases were compared with each other and with the corresponding 30-aa sequences in other human and bee HAases. The *numbers* indicate the positions of this sequence in various HAases. The *boxes* highlight the conserved (*i.e.* identical or conserved substitutions) aa between various HAases.

DISCUSSION

In this study we have identified a 30-aa sequence that is well conserved in several HAases and is required for enzyme activity of at least two human HAases (*i.e.* HYAL1 and HYAL3). The nucleotide sequence of HYAL1 gene reveals this gene contains three exons and two introns. Exons 1 (~1.5 kb) and 3 (0.9 kb) are relatively large compared with exon 2 (90 bp). The HYAL1 genomic sequence shows that the 90-bp sequence (nucleotides 1520–1609) that is missing in HYAL1v1 is the entire exon 2. Other HYAL1 variants appear to be generated by internal exon splicing events that usually involve exon 1. For example, the HYAL1wt described in this study is generated by an internal exon 1 splicing event, involving nucleotides 110 and 596. This splice variant has been described previously (GenBank™ accession number AF173154). HYAL1v2 appears to be generated by internal exon splicing involving nucleotides 109 and 952 as donor/acceptor sites, respectively, both of which are present in exon 1. Generation of HYAL1v3 variant is interesting in that it involves 2 splicing events. The first is the same internal exon 1 splicing involving nucleotides 110 and 596. The second splicing involves splicing of nucleotide 1239 present in exon 1 to nucleotide 1577 that is present in exon 2. Generation of HYAL1v4 again involves an internal exon splicing event involving exon 1; both the donor (nucleotide 108) and acceptor (nucleotide 1369) sites are present in exon 1. Generation of HYAL1v5 involves internal exon 1 splicing that starts at nucleotide 109 and ends nearly at the end of exon 1 (nucleotide 1519). Thus, the analysis of HYAL1 variants demonstrates that exon 1 in HYAL1 gene has several internal donor and acceptor sites suitable for alternative mRNA splicing resulting in the generation of various HYAL1 splice variants. In addition, exon 2 can be alternatively spliced. It is interesting to note that each of these splicing events (either internal exon splicing or splicing of two exons) maintain the same open reading frame as the HYAL1 protein, resulting in different HYAL1 variant proteins.

Our study on HYAL3 splice variants confirms that the 30-aa sequence that is important for enzyme activity is encoded by an independent exon. The nucleotide sequence of HYAL3 gene reveals that this gene contains four exons separated by three introns. Exon 3 is 90 bp in length and corresponds to the 90-bp v1 region (nucleotides 1090–1179). Thus, splicing out of the independent exon 3 generates HYAL3v1. As observed for HYAL1 variants, HYAL3v2 and HYAL3v3 splice variants are generated by an internal exon splicing events that involve exons 2 and 3. For example, HYAL3v2 variant is generated by an internal splicing event involving exon 2 (nucleotides 178–943 are deleted), and HYAL3v3 is generated by the same internal splicing event involving exon 2 and also splicing of the independent exon 3.

It is interesting to note that different bladder and lymph node specimens and cells show differences in the pattern and types of HYAL1 and HYAL3 splice variant that are expressed. The reason for this heterogeneity is unknown at present. It is noteworthy that bladder tumors show heterogeneity in their ability to progress and recur. This heterogeneity in turn relates to the differences in the biological behavior of different bladder tumors (41). It is possible that the heterogeneous expression of the HYAL1 or HYAL3 variant may be related to the different biological behavior of different bladder tumors. Because in both HYAL1 and HYAL3 proteins the loss of the 30-aa sequence results in the loss of HAase activity and because the 30-aa sequence is coded by one single independent exon, the 90-bp-long independent exon in both genes seems to encode an aa sequence that is critical for HAase activity.

Other studies involving site-directed mutagenesis of PH20, identification of a naturally occurring mutation in HYAL1, and the crystal structure of bee HAase have identified several aa present in different parts of HAase that are conserved and are important for activity (31, 35, 42). The crystal structure of bee HAase reveals that the insect and possibly mammalian HAases have a classical $(\beta/\alpha)_8$ TIM barrel structure (35). The dominant feature of the HAase structure is a large groove that extends perpendicular to the barrel axis. In bee HAase, loops following the β strands 2, 3, and 4 form one wall of the groove, and those of 1, 5, 6, and 7 form the other wall. This groove is large enough to accommodate a hexasaccharide (35). Co-crystallization of bee HAase with a hexasaccharide shows that the catalytic site that cleaves the glycosidic bond between *N*-acetyl-D-glucosamine and D-glucuronic acid lies in aa residues Asp^{143} and Glu^{145} (numbering according to GenBank™ accession number AAA27730.1). In a substrate-assisted acid-base catalytic mechanism, Glu^{145} acts as the proton donor, and the *N*-acetyl group of the substrate acts as the nucleophile. In all human HAases, this Glu residue is conserved along with Asp and is believed to be responsible for substrate cleavage (32). In the HYAL1 sequence this Glu is aa 131 (numbering according to GenBank™ accession number AAD09137.2), and in HYAL3 it is aa 129 (numbering according to GenBank™ accession number AAH12892.1). Thus, the 30-aa sequence that we have identi-

fied in HYAL1 (aa 301–300) and in HYAL3 (aa 299–328) most likely is not a part of the catalytic site.

Based on the bee HAase crystal structure, the 30-aa sequence from aa 313 to 342 (Fig. 11), that is homologous to the 30-aa sequences in HYAL1 and HYAL3, forms β sheets 6 and 7, α-helix 8, and the loops in between (35). Because the loops following β strands 6 and 7 are involved in forming one of the walls of the substrate binding groove, loss of the 30-aa sequence in HYAL1 and HYAL3 proteins may result in the loss of substrate binding. The substrate-associated catalytic cleavage of the glycosidic bond between *N*-acetyl-D-glucosamine and D-glucuronic acid requires accurate positioning of the *N*-acetyl side chain of the substrate with respect to the catalytic site (35). This is achieved by two hydrogen bonding interactions and a hydrophobic interaction. The crystal structure shows that in bee HAase, Trp^{333} is involved in hydrophobic interaction with the *N*-acetyl side chain (35). This Trp^{333} corresponds to Trp^{321} in HYAL1 and Trp^{319} in HYAL3, both of which are present in the respective 30-aa sequences (Fig. 11). This Trp residue is also conserved in all HAases and other chitinolytic enzymes (43, 44). Thus, the absence of this Trp residue in HYAL1v1 and HYAL3v1 mutant proteins may lead to improper positioning of the substrate resulting in no catalysis. It remains to be determined why this 30-aa sequence is so well conserved in various HAases and what role other conserved residues play in terms of substrate binding and catalysis. It should be noted that the loss of β sheets 6 and 7, α-helix 8, and the loops in between, because of the 30-aa deletion in HYAL1v1 and HYAL3v1, may also result in complete loss of the TIM barrel structure, making these proteins enzymatically inactive.

Other HYAL1 and HYAL3 variant proteins also illustrate the importance of various structural domains for HAase activity. For example, HYAL1v3 variant, which contains the putative catalytic site (*i.e.* Asp^{129} and Glu^{131}) but lacks aa 208–435, has no HAase activity. It is likely that the HYAL1v3 protein does not form a proper TIM barrel structure, and at the very least, it lacks the substrate-binding groove. HYAL1v2 (aa 183–435) and HYAL1v4 (aa 260–435) proteins retain the 30-aa sequence and also Glu^{268}, which has been shown to be critical for HAase activity. However, these variants are enzymatically inactive, because they lack the putative catalytic site as well as parts of the substrate-binding groove. A similar situation may hold true for HYAL3v2 variant (aa 251–435), which also does not have any HAase activity. The variants HYAL1v5 (aa 340–435) and HYAL3v3 (aa 251–435 but lacking aa 299–328) lack more than two-thirds of the respective molecules and hence will not fold properly, lack the HAase catalytic site, and have no substrate binding groove. Thus, this study illustrates the involvement of several structural domains that are conserved in various HAases and are important for enzyme activity.

Detection of various HYAL1/HYAL3 variants in bladder and prostate cancer lines, bladder tumor tissues, as well as normal kidney tissue suggest that the expression of functionally active HAase in various cells and tissues may be regulated by alternative mRNA splicing. We have previously shown that HAase levels are elevated (3–7-fold) in the urine of bladder cancer patients who have high grade (*i.e.* G2/G3) disease (39). Furthermore, in a study of 504 patients, we demonstrated that the HAase level serves as a highly sensitive (82%) and specific (83%) marker for detecting G2/G3 bladder cancer (18). Urinary HAase levels together with HA levels (*i.e.* HA-HAase test) are sensitive and specific in detecting bladder cancer and monitoring its recurrence (18, 45). We have also shown that both invasive bladder and prostate cancer cells secrete high levels of HAase activity, and HYAL1 is the major HAase expressed in these carcinomas (17, 30, 46). Consistent with these observations, in this study we observed that the full-length HYAL1wt transcript that encodes a functional HAase is expressed only in bladder and prostate cancer cells, G2/G3 bladder tumor tissues, and lymph node specimens showing tumor invasion. In normal bladder and G1 bladder tumor tissues, in a normal bladder primary culture, and in bladder tissues showing no evidence of tumor, the major HYAL1 transcript that is expressed is the HYAL1v5 variant. Because this transcript or other HYAL1 variant transcripts (*i.e.* HYAL1v2-v4) that are also expressed in some of these specimens do not encode a functional HAase, it may explain why in these tissues or cells no HAase activity and wild type HYAL1 protein are detected (30, 46, 47).

HAase protein has been shown to be associated with tumor angiogenesis and/or invasion (48). However, because HYAL1 (and also HYAL2 and HYAL3) is present on chromosome 3p 21.3 locus, and this region is a critical tumor homozygous deletion region in lung and breast cancers, it has been suggested that HYAL1 may be a tumor suppressor (7, 49). A recent study clearly demonstrates that the RASSF1 gene and not HYAL1 is the tumor suppressor gene present in that locus (50). Thus, several observations, including elevation of HAase levels in bladder and prostate tumors (18, 30), suggest that HYAL1 may have a role in promoting tumor progression. Normal cells may suppress the HAase activity of HYAL1 by generating HYAL1 splice variants that encode an inactive enzyme. It remains to be determined why the normal bladder cells/tissues, G1 bladder tumor tissues, and normal kidney tissues express different splice variants that encode inactive HYAL1 proteins.

The expression of HYAL3 protein has been previously detected in prostate cancer cells by RT-PCR analysis (51). Our results show that in all bladder tumor cells and prostate cancer cells,[2] and in all of the bladder tumor tissues that we have tested, the major HYAL3 transcript appears to be HYAL3v3 variant. This variant is enzymatically inactive. In fact we were unable to clone HYAL3wt from various cancer cells and tissues. The minor ~1.4-kb transcript expressed in cancer cells/tissues is HYAL3v1. Once again it remains unclear what is the function of these enzymatically inactive HYAL3 variant proteins.

This study identifies a 30-aa sequence that is highly conserved among all human and insect HAases and is critical for HAase activity. This study also identifies alternative mRNA splicing as the likely mechanism of regulating the expression of enzymatically active HAase in various tissues and cells. The expression of HYAL1wt mRNA that encodes the functional HYAL1 protein in high grade bladder tumor tissues and in invasive bladder/prostate cancer cells provides an insight into why HAase levels are elevated and serve as a marker for tumor progression.

Acknowledgments—We thank the University of Miami's Transplant Organ Retrieval team (Joseph Ferreira, Maximo Ariza, Michael Osorio, David Schatz, Regla Santana, and Juan Carlos Castillo) for providing normal bladder tissues. We thank Mathew Baker at ResGen™ Invitrogen Corporation for input in designing the HYAL1v1 peptide and in the generation of affinity-purified anti-HYAL1v1 IgG. We are grateful to Dr. Ian Dickerson (Department of Physiology and Biophysics) for helpful suggestions in generating stable transfectants.

REFERENCES

1. Kreil, G. (1995) *Protein Sci.* **4,** 1666–1669
2. Roden, L., Campbell, P., Fraser, J. R. E., Laurent, T. C., Petroff, H., and Thompson, J. N. (1989) *CIBA Found. Symp.* **143,** 60–86
3. Tu, A. T., and Hendon, R. R. (1983) *Comp. Biochem. Physiol. B. Comp. Biochem.* **76,** 377–383
4. Gmachl, M., and Kreil, G. (1993) *Proc. Natl. Acad. Sci. U. S. A.* **90,** 3569–3573
5. Henrissat, B. (1991) *Biochem. J.* **280,** 309–316
6. Henrissat, B., and Bairoch, A. (1996) *Biochem. J.* **316,** 695–696
7. Csoka, A. B., Frost G. I., and Stern, R. (2001) *Matrix Biol.* **20,** 499–508

[2] V. B. Lokeshwar, G. L. Schroeder, R. Carey, M. S. Soloway, and N. Iida, unpublished results.

8. Laurent, T. C., and Fraser, J. R. E. (1992) *FASEB J.* **6,** 2397–2404
9. Delpech, B., Girard, N., Bertrand, P., Chauzy, C., and Delpech, A. (1997) *J. Intern. Med.,* **242,** 41–48
10. Tammi, M. I., Day, A. J., and Turely, E. A. (2002) *J. Biol. Chem.* **277,** 4581–4584
11. Turley, E. A., Noble, P. W., and Bourguignon, L. Y. W. (2002) *J. Biol. Chem.* **277,** 4589–4592
12. Toole, B. P., Wight, T. N., and Tammi, M. I. (2002) *J. Biol. Chem.* **277,** 4593–4596
13. Ropponen, K., Tammi, M. I., Parkkinen, J., Eskelinen, M. J., Tammi, R. H., Lipponen, P. R., Argen, U. M., Alhava, E. M., and Kosma, V. M. (1998) *Cancer Res.,* **58,** 342–347
14. Setala, L. P., Tammi, M. I., Tammi, R. H., Eskelinen, M. J., Lipponen, P. R., Argen, U. M., Alhava, E. M., and Kosma, V. M. (1999) *Br. J. Cancer* **79,** 1133–1138
15. Auvinen, P., Tammi, R. H., Parkkinen, J., Tammi, M. I., Argen, U. M., Johansson, R., Hirvikoski, P., Eskelinen, M. J., and Kosma, V. M. (2000) *Am. J. Pathol.,* **156,** 529–536
16. Pirinen, R., Tammi, R., Tammi, M., Hirvikoski, P., Parkkinen, J. J., Johansson, R., Bohm, J., Hollmen, S., and Kosma V. M. (2001) *Int. J. Cancer* **95,** 12–17
17. Lokeshwar, V. B., Rubinowicz, D., Schroeder, G. L., Forgacs, E., Minna, J. D., Block, N. L., Nadji, M., and Lokeshwar, B. L. (2001) *J. Biol. Chem.* **276,** 11922–11932
18. Lokeshwar, V. B., Obek, C., Pham, H. T., Wei, D., Young, M. J., Duncan, R. C., Soloway, M. S., and Block, N. L. (2000) *J. Urol.* **163,** 348–356
19. Lokeshwar, V. B., and Block, N. L. (2000) *Urol. Clin. North Am.* **27,** 53–60
20. Liu, N., Lapcevich, R. K., Underhill, C. B., Han, Z., Gao, F., Swartz, G., Plum, S. M., Zhang, L., and Gree S. J. (2001) *Cancer Res.* **61,** 1022–1028
21. Hayen, W., Goebeler, M., Kumar, S., Riessen, R., and Nehls, V. (1999) *J. Cell Sci.* **112,** 2241–2251
22. Hobarth, K., Maier, U., and Marberger, M. (1992) *Eur. Urol.* **21,** 206–210
23. Slevin, M., Krupinski, J., Kumar, S., and Gaffney, (1998) *J. Lab. Invest.* **78,** 987–1003
24. Trochon, V., Mabilat-Pragnon, C., Bertrand, P., Legrand, Y., Soria, J., Soria, C., Delpech, B., and Lu, H. (1997) *FEBS Lett.* **418,** 6–10
25. Rooney, P., Kumar, S., Ponting, J., and Wang M. (1995) *Int. J. Cancer* **60,** 632–636
26. Lokeshwar, V. B., and Selzer, M. G. (2000) *J. Biol. Chem.* **265,** 27641–27649
27. Lokeshwar, V. B., Obek, C., Soloway, M. S., and Block N. L. (1997) *Cancer Res.* **57,** 773–777; Correction (1998) *Cancer Res.* **58,** 3191
28. Frost, G. I., Csoka, T. B., Wong, T., and Stern, R. (1997) *Biochem. Biophys. Res. Commun.* **236,** 10–15
29. Csoka, T. B., Frost, G. I., Wong, T., and Stern, R. (1997) *FEBS Lett.* **417,** 307–310
30. Lokeshwar, V. B., Young, M. J., Gouddarzi, G., Iida, N., Yudin, A. I., Cherr, G. N., and Selzer, M. G. (1999) *Cancer Res.* **59,** 4464–4470
31. Triggs-Raine, B., Salo, T. J., Zhang, H., Wicklow, B. A., and Natowicz, M. R. (1999) *Proc. Natl. Acad. Sci. U. S. A.* **96,** 6296–6300
32. Lepperdinger, G., Mullegger, J., and Kreil, G. (2001) *Matrix Biol.* **20,** 509–514
33. Cherr, G. N., Yudin, A. I., and Overstreet, J. W. (2001) *Matrix Biol.* **20,** 515–525
34. Vines, C. A., Li, M. W., Deng, X., Yudin, A. I., Cherr, G. N., and Overstreet, J. W. (2000) *Mol. Reprod. Dev.* **60,** 542–552
35. Markovic-Housley, Z., Miglierini, G., Soldatova, L., Rizkallah, P. J., and Muller, U. (2000) *Structure* **8,** 1025–1035
36. Wang, M., and Stearns, M. E. (1991) *Differentiation.* **48,** 115–125
37. Dinney, C. P. N., Fishback, R., Singn, R. K., Eve, B., Pathak, S., Brown, N., Xie, B., Fan, D., Bucana, C. D., Fidler, J. J., and Killion, J. J. (1995) *J. Urol.* **143,** 1532–1538
38. Stern, M., and Stern, R. (1992) *Matrix* **12,** 397–403
39. Pham, H. T., Block, N. L., and Lokeshwar, V. B. (1997) *Cancer Res.* **57,** 778–783; Correction (1997) *Cancer Res.* **57,** 1662
40. Shuttleworth, T. L., Wilson, M. D., Wicklow, B. A., Wilkins, J. A., and Triggs-Raine, B. L. (2002) *J. Biol. Chem.* **277,** 23008–23018
41. Lee R., Droller, M. J. (2000) *Urol. Clin. North Am.* **27,** 1–13, vii
42. Arming, S., Strobl, B., Wechselberger, C., and Kreil, G. (1997) *Eur. J. Biochem.* **247,** 810–814
43. Tews, I., Perrakis, A., Oppenheim, A., Dauter, Z., Wilson, K. S., and Vorgias, C. E. (1996) *Nat. Struct. Biol.* **3,** 638–648
44. Tews, I. Terwisscha van Scheltinga, A. C., Perrakis, A., Wilson, K. S., and Dijkstra, B. W. (1997) *J. Am. Chem. Soc.* **119,** 7954–7959
45. Lokeshwar, V. B., Schroeder, G. L., Selzer, M. G., Hautmann, S. H., Posey, J. T., Duncan, R. C., Watson, R., Rose, L., Markowitz, S., and Soloway, M. S. (2002) *Cancer* **95,** 61–72
46. Lokeshwar, V. B., Soloway, M. S., and Block, N. L. (1998) *Cancer Lett.* **131,** 21–27
47. Hautmann, S. H., Lokeshwar, V. B., Schroeder, G. L., Civantos, F., Duncan, R. C., Gnann, R., Friedrich, M. G., and Soloway, M. S. (2001) *J. Urol.* **165,** 2068–2074
48. Liu, D., Pearlman, E., Diacnou, E., Guo, K., Mori, H., Haqqi, T., Markowitz, S., Wilson, J., and Sy, M. S. (1996) *Proc. Natl. Acad. Sci. U. S. A.* **93,** 7832–7837
49. Frost, G. I., Mohapatra, G., Wong, T. M., Csoka, A. B., Gray, J. W., and Stern, R. (2000) *Oncogene* **19,** 870–877
50. Ji, L., Nishizaki, M., Gao, B., Burbee, D., Kondo, M., Kamibayashi, C., Xu, K., Yen, N., Atkinson, E. N., Fang, B., Lerman, M. I., Roth, J. A., and Minna, J. D. (2002) *Cancer Res.* **262,** 2715–2720
51. Patel, S., Turner, P. A., Stubberfield, C., Barry, E., Rohlff, C. R., Stamps, A., Tyson, K., Terrett, J., Box, G., Eccles, S., and Page, M. J. (2002) *Int. J. Cancer* **97,** 416–424

EVALUATION OF THE PROGNOSTIC POTENTIAL OF HYALURONIC ACID AND HYALURONIDASE (HYAL1) FOR PROSTATE CANCER: A FIVE-YEAR STUDY

J. Timothy Posey[1], Mark S. Soloway[1], Sinan Ekici[1], Mario Sofer[1], Francisco Civantos[1],

Robert C. Duncan[2], Vinata B. Lokeshwar[1,3]*

Departments of Urology[1], Department of Epidemiology[2], and Cell Biology and Anatomy[3], University of Miami School of Medicine, Miami, Florida 33101.

RUNNING TITLE: HA and HAase as prognostic indicators for prostate cancer

*: **Address for correspondence:**
Vinata B. Lokeshwar, Ph.D.
Department of Urology (M-800)
University of Miami School of Medicine
P.O. Box 016960
Miami, Florida, 33101

Phone: (305) 243-6321

Fax: (305) 243-6893

e-mail: vlokeshw@med.miami .edu

Key words: Prostate cancer, prognostic indicators, hyaluronic acid, hyaluronidase, HYAL1

Abbreviations used: CaP: prostate cancer/cancer of the prostate; **EPE:** extra-prostatic extension; **HA:** hyaluronic acid; **HAase:** hyaluronidase; **IHC:** immunohistochemistry /immunohistochemical; **PSA:** Prostate specific antigen.

Support: Department of Defense grant DAMD 170210005; NCI grant RO1 CA 72821; Sylvester Comp. Cancer Center, and Department of Urology, University of Miami.

ABSTRACT

Despite the development of nomograms designed to evaluate a prostate cancer (CaP) patient's prognosis, the information has been limited to prostate specific antigen (PSA), clinical stage, Gleason score and tumor volume estimates. To improve our ability to predict prognosis, information regarding the molecular properties of CaP is needed. Hyaluronic acid (HA) is a glycosaminoglycan that promotes tumor metastasis. Hyaluronidase (HAase) is an enzyme that degrades HA into angiogenic fragments. We recently (Lokeshwar et al J. Biol. Chem. 276: 11922-32; 2001) showed that in CaP tissues, while HA is localized mostly in the tumor-associated stroma, HYAL1 type HAase is exclusively localized in CaP cells. We evaluated the prognostic potential of HA and HYAL1 in CaP by immunohistochemistry.

Archival CaP specimens were obtained from patients who underwent radical retropubic prostatectomy for clinically localized CaP. Group 1 (n = 25): Patients who showed biochemical recurrence (PSA > 0.4 ng/ml; mean recurrence: 21.3 mos). Group 2: no clinical or biochemical recurrence patients (n = 45, mean follow-up: 80.9 mos). For HA and HYAL1 staining, a biotinylated HA-binding protein and an anti-HYAL1 antibody were used. The staining was evaluated on the basis of intensity (0 to 3+) and as dense or sparse (for HA staining only) and then grouped as low-grade and high-grade.

In CaP specimens, HYAL1 was exclusively expressed in tumor cells. Although, the stroma was stained positive for HA, 40% of tumor cells also expressed HA. HA, HYAL1, and combined HA-HYAL1 staining predicted progression with 96%, 84% and 88% sensitivity, 55.5%, 80% and 84.4% specificity and 70%, 81.4% and 85.7% accuracy, respectively. In the univariate analysis, preoperative PSA, Gleason sum, stage, margin, seminal vesicle, extra-prostatic extension (EPE), HA, HYAL1 and HA-HYAL1 were significant in predicting progression ($P < 0.05$). However, in the multiple logistic regression analysis, only EPE (odds ratio (OR) = 33.483; P, 0.002), HYAL1 (OR =12.42; p = 0.009)/HA-HYAL1 (OR = 18.048; P = 0.0033) and margin (OR = 26.948; P = 0.006) were significant. Thus, in this 5-year follow-up study, HYAL1 together, with EPE and margin was found to be an independent prognostic indicator.

INTRODUCTION

In the last decade, due to the increased public awareness of serum prostate specific antigen (PSA) screening, the number of prostate cancer (CaP) cases has steadily increased. PSA screening has resulted in the detection of more clinically localized CaP, which has the potential to be cured by radical prostatectomy or radiation therapy (1-4). However, within the first 10 years following surgery, CaP recurs (defined as PSA failure (biochemical relapse), local/systemic recurrence) in about 10-50% of cases depending upon a variety of prognostic factors (5-7). Treatment failure may be due to a local recurrence or distant metastasis. Existing pre-operative indicators (i.e., PSA levels, clinical stage, biopsy Gleason sum) or their combination in nomograms, as well as, surgical and pathologic parameters (i.e., prostatectomy Gleason sum, margin +/-, node status and seminal vesicle and extra-prostatic extension (EPE)) provide a limited estimate of the prognosis for CaP (8,9). Identifying molecules that are expressed in clinically localized CaP but associate with CaP invasion and metastasis might significantly improve the prognostic capabilities and management of CaP patients following a curative approach. We have recently shown the expression of two tumor markers, hyaluronic acid (HA) and hyaluronidase (HAase) in CaP (10,11).

HA is a glycosaminoglycan, made up of repeated disaccharide units D-glucuronic acid and N-acetyl-D-glucosamine (12-14). It is a component of tissue matrix and tissue fluids. HA keeps the tissues hydrated and maintains the osmotic balance (12-14). In addition, by interacting through cell surface receptors (e.g., CD44 and RHAMM) it regulates cell adhesion, migration and proliferation (15). Concentrations of HA are elevated in several cancers including colon, breast, prostate, bladder and lung and serve as a highly sensitive and specific marker for detecting bladder cancer, regardless of the tumor grade (16-24). In tumor tissues, HA promotes tumor metastasis by opening up spaces for tumor cells to migrate and actively supports tumor cell migration by interacting with cell surface HA receptors (12,14,15). An HA coat around tumor

cells may offer some protection against immune surveillance and cause a partial loss of contact-mediated inhibition of cell growth and migration (25-28). Localization of HA either in tumor-associated stroma or tumor cells depends upon the tissue origin. For example, in colon and stomach cancers, most of the tumor cells express HA (17,21). In bladder cancer, HA expression is equally distributed in tumor-stroma and tumor cells (16). However, in CaP HA is mostly localized in tumor stroma (22).

HAase is an endoglycosidase that degrades HA into small angiogenic fragments of 3-25 disaccharide units (29,30). Angiogenic HA fragments induce endothelial cell proliferation, adhesion and migration by activating focal adhesion kinase and MAP kinase pathways (31,32). We have previously shown the presence of angiogenic HA fragments in high Gleason sum (≥ 7) CaP tissues (10). Six HAase genes have been identified in humans. Among these, products of HYAL1, HYAL2 and PH20 are well characterized (33-35). We have shown that HYAL1 type HAase is the major HAase expressed in prostate and bladder cancer tissues and have characterized the expression of HYAL1 at the mRNA and protein levels in prostate and bladder tumor cells (11,36,37). The HAase expressed by CaP cells has the same pH activity profile as that of HYAL1 (10). The expression of PH20 mRNA has been detected by RT-PCR analysis in some tumor tissues including CaP, however, the presence of PH20 protein has not been documented in these studies (38,39). Since our recent observations show that HAase family of genes are extensively alternative spliced, which in turn, regulates the generation of enzymatically active HAases, characterization of HAase expression in tumor tissues at the protein level may be necessary (40). By immunohistochemical techniques we have previously shown that the HYAL1 type HAase is localized in tumor epithelial cells and the expression increases with higher grades of CaP (10).

In this study, we examined the prognostic potential of HA and HYAL1 for predicting CaP progression by immunohistochemically localizing these markers in archival CaP tissues and correlating the staining intensity with PSA biochemical recurrence as an indicator of CaP progression.

MATERIALS AND METHODS

Specimens and study individuals: Seventy-three CaP specimens were obtained from patients who underwent radical retropubic prostatectomy for clinically localized CaP and were followed for recurrence/disease progression. Three out of the total 73 specimens were not included in the final analysis since those patients had positive lymph nodes. On all of the patients a minimum follow-up of 64 months was available. This study was conducted under a protocol approved by the Institutional Review Board of University of Miami. Progressed group of patients (n = 25) includes those who had biochemical recurrence (PSA > 0.4 ng/ml) within 64 months (mean time to recurrence = 21.3 months; range 3 to 61 months). Non-progressed group includes patients (n = 45) who were disease free (i.e., no clinical or biochemical recurrence) for a minimum of 64 months (mean follow-up 80.6 months; range 64 – 114 months). The patient characteristics with respect to age, pre-operative PSA and tumor (i.e., Gleason, stage, margin, EPE, seminal vesicle invasion) are shown in Table 1.

Immunohistochemistry (IHC): IHC localization of HA and HYAL1 in CaP tissues was carried out as described previously (10). For all specimens, paraffin-embedded blocks containing CaP tissues representing the majority of the Gleason sum were selected by the study 's pathologist (FC). The blocks were cut into 3-μm thick sections and placed on positively charged slides. The specimens were deparafinized, rehydrated and treated with an Antigen-retrieval solution (Dako Laboratories). For each specimen, two slides were prepared, one for HA and the other for HYAL1 staining. For HA staining, the slides were incubated with 2 μg/ml of a biotinylated bovine nasal cartilage protein at room temperature for 35 min (10). The specificity of HA staining was established as described previously (10). Following incubation with the HA-binding protein, the slides were washed in phosphate buffered saline (PBS) and sequentially incubated with streptavidin peroxidase at room temperature for 30 min and 3,3-diaminobenzidine (DAB)

chromogen substrate solution (Dako Laboratories). The slides were counterstained with hematoxylin, dehydrated and mounted.

For HYAL1 staining, the slides were incubated with 3.7 μg/ml of anti-HYAL1 IgG at 4^0 C for 16 hr. Rabbit polyclonal anti-HYAL1 IgG was generated against a peptide sequence present in HYAL1 protein (amino acids 321 to 338) and its specificity for IHC was confirmed as described previously (10, 37). Following incubation with anti-HYAL1 IgG, the slides were washed in PBS and incubated with a linking solution containing a biotinylated goat anti-rabbit IgG (Dako LSAB kit) at room temperature for 30 min. The slides were then treated with streptavidin peroxidase and DAB chromogen. The slides were counterstained with hematoxylin, dehydrated and mounted.

Slide grading: Two readers (JTP and VBL) independently evaluated all slides in a blinded fashion. Any discrepancy in assigning staining intensity was resolved by both readers reexamining those slides simultaneously. The staining for HA and HYAL1 was graded as 0 (no staining), 1+, 2+ and 3+. For HA staining, in each slide, both the tumor-associated stroma and tumor cells were graded separately for staining intensity. In case of HA staining, the stromal staining was also evaluated as dense or sparse. The overall staining grade for each slide was assigned based on the staining intensity of the majority of the tumor tissue in the specimen. However, if approximately 50% of the tumor tissue stained as 1+ and the other 50% as 3+, the overall staining grade was 2+. If the staining distribution was, approximately 50% of the tumor staining 2+ and the remaining staining as 3+, the overall staining inference was assigned as 3+. The staining scale was further subcategorized into low-grade and high-grade.

For HA staining, low-grade includes 0, 1+ sparse and 2+ sparse/dense staining and high-grade staining includes 3+ sparse and 3+ dense staining. In those cases (n=2), where the stromal tissues were evaluated as low-grade staining but the tumor cells stained as 3+, the overall HA staining was considered as high-grade. For HYAL1, high-grade staining represents, 2+ and 3+ staining, whereas, low-grade staining includes 0 and 1+ staining intensities. For the combined HA-HYAL1 staining, a positive result was indicated only when both HA (stromal, tumor cells or both) and HYAL1 staining intensities were of high-grade. Any other combination was considered as negative.

High-grade staining was considered as a true positive result and the low-grade staining indicated a false negative result if the patient had biochemical recurrence. If the patient had no clinical/biochemical recurrence, the low-grade staining indicated a true negative result and the high-grade staining, was taken as a false positive result.

Statistical analysis: The sensitivity, specificity, accuracy, positive predictive value (PPV) and negative predictive value (NPV) for HA, HYAL1 and HA-HYAL1 staining inferences were calculated using the 2 x 2 contingency table (high-grade/low-grade staining and progressed/ non-progressed CaP patients). The data on various, biochemical, surgical and pathologic parameters, as well as HA, HYAL1 and HA-HYAL1 staining inferences were analyzed by univariate logistic regression analysis. The data were also analyzed by a forward stepwise multiple logistic regression analysis beginning with all of the potential predictor variables. Statistical analysis was carried out by project's statistician (RCD) using SAS Software Program (version 8.02, SAS Institute, NC).

RESULTS

HA Localization: HA was localized in 70 archival CaP specimens obtained from patients who underwent radical retropubic prostatectomy for clinically localized disease. These patients were being monitored for disease progression. A Rise in PSA $\geq$ 0.4 ng/ml was taken as an indicator of biochemical recurrence (either local recurrence or systemic progression). A minimum follow-up of 64 months was available for all patients. HA was localized in CaP tissues using a biotinylated HA binding protein. Fig. 1 shows HA staining in Gleason sum 6 (A, B) 7 (C, D) and 8 (E, F) CaP specimens from non-progressed (A, C, E) and progressed (B, D, F) patients. In all of the CaP specimens HA is localized mostly in the tumor-associated stroma, although some

tumor cells also show HA staining in CaP specimens from patients who progressed (panels B and F).

As shown in Fig. A, C, and E the CaP specimens from non-progressed patients have low-grade HA staining, regardless of the Gleason sum. Out of the 45 patients free of recurrence, 26 had low-grade HA staining. However, the CaP specimens from the patients who progressed in < 64 months (median time to recur = 19 months; mean time to recur = 21.3 months), show high-grade HA staining (Panels B, D, F). Out of the 25 CaP specimens from progressed patients, 22 showed high-grade staining in tumor stroma; 8 of these 22 also showed high-grade HA staining in tumor cells. In addition, 2 of the 25 CaP specimens showed high-grade staining only in tumor cells. Fig. 2 shows an example of tumor cells that are positive for high-grade HA staining. Tumors cells appear to stain for HA equally, both in the cytoplasm and plasma membrane (Fig. 2 B, magnified view). Thus, out of the 25 CaP specimens from progressed patients, 24 showed high-grade HA staining either in tumor stroma, tumor cells or both. Thus, high-grade HA staining (stroma, tumor cells or both) has 96% sensitivity, 55.5% specificity, 70% accuracy, 54.5% PPV and 96.2% NPV for predicting the biochemical recurrence (Table 2).

HYAL1 localization: An anti-HYAL1 peptide IgG was used to localize HYAL1 in the archival CaP specimens. Fig. 3 shows HYAL1 localization in Gleason 6 (A, B), 7 (C, D) and 8 (E, F) CaP tissues from patients who did not (A, C, E) and who did (B, D, F) progress. As shown in Fig. 3, low-grade HYAL1staining is seen in all 3 CaP specimens from patients who did not progress, regardless of their Gleason sum (Fig. 3, panels A, C and E). Among the 45 non-progressed patients, Cap specimens of 36 patients showed low-grade HYAL1 staining. In CaP specimens from progressed patients, tumor cells, and not tumor-stroma, stain for HYAL1. All 3 CaP specimens from progressed patients show high-grade HYAL1 staining (Fig. 3, panels B, D and F), regardless of their Gleason sum. Out of the 25 progressed patients, CaP specimens from 21 patients showed high-grade HYAL1 staining. Thus, in this cohort of 70 patients, the HYAL1 localization in CaP specimens has 84% sensitivity, 82.2% specificity, 82.9% accuracy, 70% PPV and 90.2% NPV for predicting biochemical recurrence within 64 months (Table 2).

Combined HA-HYAL1 staining: We next determined the ability of combined high-grade HA and HYAL1 staining to predict biochemical recurrence. The combined HA-HYAL1 staining has 84% sensitivity, 86.7% specificity, 85.7% accuracy, 77.8% PPV and 90.7% NPV for predicting progression. When 64 months was used as a cut-off limit to evaluate progression, there were 7 false positive cases, i.e., the specimens showed high-grade HA and HYAL1 staining but the patients had no disease recurrence within 64 months. However, among these 7 false positive cases, 2 had a biochemical recurrence at 70 months (Table 2).

Evaluation of the prognostic capabilities of pre-operative, post-operative parameters and HA and HYAL1 staining inferences:

Univariate analysis: We performed a univariate logistic regression analysis to determine the prognostic significance of pre-operative parameters (i.e., age, PSA and clinical stage), post-operative surgical and pathologic parameters (i.e., Gleason sum, margin +/-, EPE, seminal vesicle invasion +/-), as well as, inferences of HA, HYAL1 and combined HA-HYAL1 staining. As shown in Table 3, both age (P= 0.297; odds ratio (OR) = 1.041) and stage (P = 0.287; OR = 1.714) are not significant in predicting biochemical recurrence in the univariate analysis. However, pre-operative PSA (P = 0.0174; OR = 1.10), Gleason sum (P = 0.0023; OR = 3.062); positive margin (P = 0.0001; OR = 9.0), EPE (P < 0.0001; OR = 34.125), seminal vesicle invasion (P <0.0001; OR = 17.818), HA staining (P = 0.0014, OR = 30), HYAL1 staining (P < 0.0001; OR = 24.28) and combined HA-HYAL1 staining (P < 0.0001; OR = 34.125) are found to be significant in predicting biochemical recurrence. Patients with Gleason sum ≥ 7 have been shown to have a greater risk of progression (41). In the univariate analysis, Gleason sum ≥ 7 patients had 2.3-fold greater odds of developing biochemical recurrence (P = 0.015; OR = 6.982) than when CaP tissues all Gleason sums were analyzed together (Table 3).

Forward stepwise multiple logistic regression analysis: To determine the smallest number of variables that can jointly predict biochemical recurrence in this cohort of study patients, we performed the forward stepwise multiple logistic regression analysis. Initially, when age, pre-operative PSA, clinical stage, Gleason sum, EPE, seminal vesicle invasion, HA staining and HYAL1 staining were included in the model, only EPE (P = 0.0023; OR = 33.483), positive margin (P = 0.0059; OR = 26.948), HYAL1 staining (P = 0.0094; OR = 12.423) reached statistical significance in predicting biochemical recurrence (Table 4 a). Gleason sum did not reach statistical significance in the multiple logistic regression analysis even after the patients were stratified according to Gleason ≥ 7 and < 7 (data not shown).

The inclusion of the combined HA-HYAL1 staining inference instead of the individual HA and HYAL1 staining inferences, in the multiple regression model, again showed that EPE (P = 0.0023; OR = 35.944), margin (P = 0.0086; OR = 24.438) and HA-HYAL1 staining (P = 0.0033; OR = 18.047) were significant in predicting biochemical recurrence. None of the other routine prognostic parameters (i.e., age, PSA, clinical stage, Gleason sum (or Gleason stratification as Gleason ≥ 7 and < 7 and seminal vesicle invasion) that were included in the model reached statistical significance (i.e., $P > 0.05$ in each case).

DISCUSSION

In this study we demonstrate for the first time that HYAL1 and combined HA-HYAL1 staining inferences provide independent prognostic information for predicting CaP recurrence/ progression, over and above the prognostic information provided by the standard pre and post-operative parameters. Radical prostatectomy for organ-confined disease is performed with the idea of disease cure (42,43). However, disease relapses in high percentage of cases despite careful selection of patients for surgery based on individual pre-operative parameters or their combination in algorithms and nomograms (6). Certain genes and their products that associate with CaP growth and metastasis have shown potential in predicting biochemical recurrence following surgery (8; 44). Since both HA and HYAL1 are likely to be involved in tumor metastasis and angiogenesis (45-50), it is not surprising that we found HA, HYAL1 and combined HA-HYAL1 staining inferences to have prognostic significance in predicting biochemical recurrence. It is noteworthy that, although in this study we eliminated 3 CaP specimens from patients who had positive lymph nodes, all showed high-grade HA and HYAL1 staining, suggesting again that these molecules are associated with CaP progression.

In this study, HA staining in CaP tissues had high sensitivity (96%) but low specificity (55.5%) in predicting biochemical recurrence. Consequently, although in the univariate analysis, HA staining showed prognostic significance (Table 3), in the forward stepwise multiple logistic regression analysis, it had no additional prognostic significance when standard biochemical, surgical and pathologic parameters, as well as, HYAL1 staining were included in the model (Table 4). Consistent with this observation, Lipponen et al previously reported that HA expression in tumor-stroma of CaP specimens has no additional prognostic significance over the standard prognostic indicators (i.e., Gleason sum, stage and node status) (22). The combination of HA with HYAL1 did increase the specificity, accuracy and PPV of the combination when compared to that of HYAL1 or HA alone (Table 2). Similarly, the odds ratio of the HA-HYAL1 combination (18.047) was slightly better than that of HYAL1 (12.423) alone. Thus, HA staining of CaP tissues may have some significance in predicting biochemical, however, it is clearly not as good of a prognostic indicator as HYAL1.

Lipponen et al also reported that 39% of the CaP specimens expressed HA in tumor cells, in addition to the expression in tumor-stroma. However, the presence of HA in tumor cells did not have independent prognostic significance (22). In our study, although we found 40% of the CaP specimens from progressed patients showed high-grade HA staining in tumor cells, it

did not have any independent prognostic significance. In contrast to these observations, in gastrointestinal, colon and breast cancers, HA expression in tumor cells correlates with poor survival (17,18,21). Thus, although HA expression is elevated in many types of cancers, the clinical significance of this expression, in terms of predicting prognosis, varies with the tissue of origin of each cancer.

We have shown that HAase levels, measured using an ELISA-like assay correlate with CaP progression and serve as an accurate urine marker for detecting intermediate- and high-grade bladder cancer (11,51). HYAL1 is expressed in invasive CaP and bladder cancer cells (11,36,37). The present study is the first to demonstrate the prognostic significance of HYAL1 expression in cancer. In this study, HYAL1 staining in CaP specimens has high sensitivity (84%), specificity (82.2%) and accuracy (82.9%) in predicting biochemical recurrence following radical prostatectomy. Among all of the pre- and post-operative prognostic parameters included in the forward stepwise multiple logistic regression analysis, only EPE and margin have additional prognostic significance, if HYAL1 is included in the model (Table 4). Our observations are also consistent with a recent observation that over-expression of HYAL1 induces metastasis in a human xenograft model involving PC3-M CaP cells (52). Taken together, HYAL1 is a tumor cell-derived hyaluronidase whose expression associates with cancer progression.

In this study, all of the patients had a minimum follow-up of 64 months and a median follow-up of 79 months in the non-progressed group. Greater than 5-year follow-up duration is long enough if any of the CaP patients placed in the non-progressed category were to have a biochemical recurrence. Therefore, based on this first report, with sufficiently long follow-up, it is safe to suggest that HYAL1 either alone, or in combination with HA, is useful in predicting biochemical recurrence following radical prostatectomy. Most CaP patients with clinically localized disease have pre-operative PSA between 4 and 10 ng/ml, stage T1C disease and a biopsy Gleason between 5 and 7 (8). Such similarity limits the prognostic capability of these pre-operative parameters. Further studies on HYAL1 and HA-HYAL1 staining in biopsy specimens should reveal whether these markers could improve our ability to predict prognosis for patients who choose a curative approach involving radical prostatectomy.

Acknowledgments: We thank Dr. Anil Vaidya for helping in gathering some of the follow-up information. We thank Ms. Pamela Roza for her help with the illustrations.

REFERENCES:

1. Etzioni, R., Penson, D.F., Legler, J.M., di Tommaso, D., Boer, R., Gann, P.H., Feuer, E.J. Overdiagnosis due to prostate-specific antigen screening: lessons from U.S. prostate cancer incidence trends. J Natl Cancer Inst. 94: 981-990, 2002.
2. Yao, S.L., Lu-Yao, G. Understanding and appreciating overdiagnosis in the PSA era. J Natl Cancer Inst. 94:958-960, 2002
3. Muzzonigro, G., Galosi, A.B. Biological selection criteria for radical prostatectomy. Ann N Y Acad Sci. 963:204-212, 2002.
4. Small, E.J., Roach M 3rd. Prostate-specific antigen in prostate cancer: a case study in the development of a tumor marker to monitor recurrence and assess response. Semin Oncol. 29: 264-73, 2002.
5. Palisaan, R.J., Graefen, M., Karakiewicz, P.I., Hammerer, P.G., Huland, E., Haese, A., Fernandez, S., Erbersdobler, A., Henke, R.P., Huland, H. Assessment of clinical and pathologic characteristics predisposing to disease recurrence following radical prostatectomy in men with pathologically organ-confined prostate cancer. Eur Urol. 41:155-161, 2002.
6. Waltregny, D. de Leval, L., Coppens, L., Youssef, E., de Leval, J., Csatronovo, V. Detection of the 67-kD laminin receptor in prostate cancer biopsies as a predictor of recurrence after radical prostatectomy. Eur. Urol., 40: 495-503, 2002.

7. Pound CR, Partin AW, Epstein JI, Walsh PC. Prostate-specific antigen after anatomic radical retropubic prostatectomy. Patterns of recurrence and cancer control. Urol Clin North Am. 24: 395-406, 1997.
8. Pettaway, C.A. Prognostic markers in clinically localized prostate cancer. Tech. Urol., 4: 35-42, 1998.
9. Blute, M.L. Bergstralh, E.J., Iocca, A., Scherer, B., Zincke, H. Use of Gleason score, prostate specific antigenm seminal vesicle and margin status to predict biochemical failure after radical prostatectomy. J. Urol., 165: 119-125, 2001.
10. Lokeshwar, V.B., Rubinowicz, D., Schroeder, G.L., Forgacs, E., Minna, J.D., Block, N.L. Nadji, M., Lokeshwar, B.L. Stromal and epithelial expression of tumor markers hyaluronic acid and hyaluronidase in prostate cancer. J. Biol. Chem. 276: 11922-11932, 2001.
11. Lokeshwar, V.B., Lokeshwar, B.L., Pham, H.T., Block, N.L. Association of hyaluronidase, a matrix-degrading enzyme, with prostate cancer progression. Cancer Res., 56: 651-657, 1996.
12. Tammi, M.I., Day, AJ, Turley, EA. Hyaluronan and homeostasis: a balancing act. J. Biol. Chem. 277: 4581-4584, 2002.
13. Tool, BP. Hyaluronan is not just a gloo! J. Clin. Invest. 106: 335-336, 2000.
14. Delpech, B., Girard, N., Bertrand, P., Courel, N.M., Chauzy, C., Delpech, A. Hyaluronan: Fundamental principles and applications in cancer. J. Intern. Med. 242: 41-48, 1997.
15. Turley EA, Noble PW, Bourguignon LY. Signaling properties of hyaluronan receptors. J Biol Chem. 277: 4589-4592, 2002.
16. Hautmann, S.H., Lokeshwar, V.B., Schroeder, G.L., Civantos, F., Duncan, R.C., Friedrich, M.G., Soloway, M.S. Elevated tissue expression of hyaluronic acid and hyaluronidase validate HA-HAase urine test for bladder cancer. J. Urol., 165: 2068-2074, 2000.
17. Setala, L.P., Tammi, M.I., Tammi, R.H., Eskelin, M.J., Lipponen, P.R., Argen, U.M., Parkkinen, J., Alhava, E.M., Kosma, V.M., Hyaluronan expression in gastric cancer cells is associated with local and nodal spread and reduced survival rate. Br. J. Cancer, 79: 1133-1138, 1999.
18. Auvinen, P., Tammi, R., Parkkinen, J., Tammi, M., Agren, U., Johansson, R., Hirvikoski, P., Eskelinen, M., Kosma, V.M., Hyaluronan in peritumoral stroma and malignant cells associates with breast cancer spreading and predicts survival. Am. J. Pathol., 156: 529-536, 2000.
19. Pirinen, R., Tammi, R., Tammi, M., Hirvikoski, P., Parkkinen, J.J., Johansson, R. Prognostic value of hyaluronan expression in non-small-lung cancer: increased stromal expression indicates unfavorable outcome in patients with adenocarcinoma. Int J Cancer 95: 12-27, 2001.
20. Knudson, W. Tumor associated hyaluronan: providing an extracellular matrix that facilitates invasion. Am. J. Pathol., 148: 1721-1726, 1996.
21. Ropponen, K., Tammi, M., Parkkinen, J., Eskelinen, M., Tammi, R., lipponen, P., Argen, V., Alhava, E., Kosma, V.M. Tumor-associated hyaluronan as an unfavorable prognostic factor in colorectal cancer. Cancer Res., 58:342-347, 1998.
22. Lipponen, P., Aaltomaa, S., Tammi, R., Tammi, M., Agren, U., Kosma, V.M. High stromal hyaluronan level is associated with poor differentiation and metastasis in prostate cancer. Eur. J. Cancer 37: 849-856, 2001.
23. Lokeshwar, V.B., Obek, C., Pham, H.T., Wei, D.C., Young, M.J., Duncan, R.C, Soloway, M.S., Block, N.L. Urinary hyaluronic acid and hyaluronidase: Markers for bladder cancer detection and evaluation of grade. J. Urol., 163: 348-356, 2000.
24. Lokeshwar, V.B., Obek, C., Soloway, M.S., Block, N.L. Tumor-associated hyaluronic acid: A new sensitive and specific urine marker for bladder cancer. Cancer Res., 57: 773-777, 1997.
25. Liu N., Lapcevich, R.K., Underhill, C.B., Han, Z., Gao, F., Swartz, G., Plum, S.M., Zhang, L., Gree, S.J. Metastatin: a hyaluronan-binding complex from cartilage that inhibits tumor growth. Cancer Res. 61:1022- 1028, 2001.
26. Hayen, W., Goebeler, M., Kumar, S., Riessen, R., Nehls, V. Hyaluronan stimulates tumor cell migration by modulating the fibrin fiber architecture. J Cell Sci. 112: 2241-251, 1999.
27. Hoborth, K., Maier, U., Marberger, M., Topical chemoprophylaxis of superficial bladder cancer by mitomycin C and adjuvant hyaluronidase. Eur. Urol., 21: 206-210, 1992.

28. Itano, N., Atsumi, F., Sawai, T., Yamada, Y., Miyaishi, O., Senga, T., Hamguchi, M., Kimata, K. Abnormal accumulation of hyaluronan matrix diminishes contact inhibition of cell growth and promotes cell migration. Proc. Natl. Acad. Sci. 99: 3609-3614, 2002.
29. Roden, L., Campbell, P., Fraser, J.R.E., Laurent, T.C., Petroff, H., Thompson, J.N. Enzymatic pathways of hyaluronan catabolism. In: The biology of hyaluronan. Whelan, E, (ed), Wiley, Chichister, Ciba Foundation Symp., 143, pp-60-86, 1989.
30. Jedrzejas, M.J. Structural and functional comparison of polysaccharide-degrading enzymes. Crit Rev Biochem Mol Biol.35: 221-251, 2000.
31. West, D.C., Hampson, I.N., Arnold, F., Kumar, S. Angiogenesis induced by degradation products of hyaluronic acid. Science, 228: 1324-1326, 1985.
32. Lokeshwar, V.B., Selzer, M.G. Differences in hyaluronic acid-mediated functions and signaling in arterial, microvessel, and vein-derived human endothelial cells. J. Biol. Chem., 275: 27641-27649, 2000.
33. Csoka, A.B., Frost, G.I., Stern, R. The six hyaluronidase-like genes in the human and mouse genomes. Matrix Biol. 20: 499-508, 2001.
34. Lepperdinger, G., Mullegger, J., Kreil, G. Hyal2--less active, but more versatile? Matrix Biol. 20: 509-514, 2001.
35. Cherr, G.N., Yudin, A.I., Overstreet, J.W. The dual functions of GPI-anchored PH-20: hyaluronidase and intracellular signaling. Matrix Biol. 20: 515-525, 2001.
36. Lokeshwar, V.B., Soloway, M.S., Block, N.L. Secretion of bladder tumor-derived hyaluronidase activity by invasive bladder cancer cells. Cancer Lett., 131: 21-27, 1998.
37. Lokeshwar, V.B., Young, M.J., Goudarzi, G., Iida, N., Yudin, A.I., Cherr, G.N., Selzer, M.G., Identification of bladder tumor-derived hyaluronidase: Its similarity to HYAL1. Cancer Res., 59: 4464-4470, 1999.
38. Godin, D.A., Fitzpatrick, P.C., Scandurro, A.B., Belafsky, P.C., Woodworth, B.A., Amedee, R.G., Beech, D.J., Beckman, B.S. PH20: a novel tumor marker for laryngeal cancer. Arch. Otolaryngol Head Neck Sug., 126: 402-404, 2000.
39. Beech, D.J., Madan, A.K., Deng, N. Expression of PH-20 in normal and neoplastic breast tissue. J Surg Res. 103: 203-207, 2002.
40. Lokeshwar, V.B. Schroeder, G.L., Carey, R.I. Soloway, M.S., Iida, N. Regulation of hyaluronidase activity by alternative mRNA splicing. J. Biol. Chem. 2002 (In Press).
41. Sweat, S.D., Bergstralh, E.J., Slezak, J., Blute, M.L., Zincke, H. Competing risk analysis after radical prostatectomy for clinically nonmetastatic prostate adenocarcinoma according to clinical Gleason score and patient age. J Urol. 168: 525-529, 2002.
42. Fradet, Y. Role of radical prostatectomy in high-risk prostate cancer. Can J Urol. 9: 8-13 2002.
43. Klein, E.A., Kupelian, P.A. Localized prostate cancer. Curr Treat Options Oncol. 1: 433-445, 2000.
44. Isaacs W, De Marzo A, Nelson W. Focus on prostate cancer. Cancer Cell. 2:113-116, 2002.
45. Muzzonigro, G., Galosi, A.B. Biological selection criteria for radical prostatectomy. Ann N Y Acad Sci. 963:204-212, 2002.
46. Feroze-Merzoug, F,, Schober, M.S., Chen, Y.Q. Molecular profiling in prostate cancer. Cancer Metastasis Rev. 20: 165-171, 2001.
47. Claudio, P.P., Zamparelli, A., Garcia, F.U., Claudio, L., Ammirati, G., Farina, A., Bovicelli, A., Russo, G., Giordano, G.G., McGinnis, D.E., Giordano, A., Cardi, G. Expression of Cell-Cycle-regulated Proteins pRb2/p130, p107, p27(kip1), p53, mdm-2, and Ki-67 (MIB-1) in Prostatic Gland Adenocarcinoma. Clin Cancer Res. 8: 1808-1815, 2002.
48. Asmann, Y.W., Kosari, F., Wang, K., Cheville, J.C., Vasmatzis, G. Identification of differentially expressed genes in normal and malignant prostate by electronic profiling of expressed sequence tags. Cancer Res. 62: 3308-3314, 2002.
49. Vis, A.N., van Rhijn, B.W., Noordzij, M.A., Schroder, F.H., van der Kwast, T.H. Value of tissue markers p27(kip1), MIB-1, and CD44s for the pre-operative prediction of tumour features in screen-detected prostate cancer. J Pathol. 197: 148-154, 2002.
50. Ross, J.S., Sheehan, C.E., Fisher, H.A., Kauffman, R.A., Dolen, E.M., Kallakury, B.V. Prognostic markers in prostate cancer. Expert Rev Mol Diagn. 2: 129-142, 2002.

51. Pham, H.T., Block, N.L., Lokeshwar, V.B. Tumor derived hyaluronidase: a diagnostic urine marker for high-grade bladder cancer. Cancer Res., 57: 778-783, 1997.
52. Patel, S., Turner, P.R., Stubberfield, C., Barry, E., Rohlff, C.R., Stamps, A., McKenzie, E., Young, K., Tyson, K., Terrett, J., Box, G., Eccles, S., Page, M.J. Hyaluronidase gene profiling and role of hyal-1 overexpression in an orthotopic model of prostate cancer. Int J Cancer. 97: 416-24, 2002.

Table 1: Distribution of pre- and post-operative parameters among study patients. Note that biochemical recurrence with post-operative PSA levels ≥ 0.4 ng/ml within 64 months was used a cut point for defining progression. Thus, any CaP patient who showed a biochemical recurrence within 64 months was included in the progressed category. Progressed group: Median time to recur is 19 months and mean time to recur is. 21.3 months. Non-progressed group: Median follow-up 79 months. Mean follow-up 80.6 months.

	Age (Years)	PSA (ng/ml)	Clinical Stage	Gleason Sum	EPE	Margin	Seminal Vesicle
Progression	Pre-operative parameters			Post-operative parameters			
Biochemical recurrence (n = 25)	Median: 64 Mean: 65.1 Range: 51-74	Median: 9.0 Mean: 14.04 Range:2- 62	T1 C = 10 T2 A = 5 T2 B = 10	6 = 2 7 = 14 8 = 6 9 = 3	(+) = 21 (-) = 4	(+) = 18 (-) = 7	(+) = 14 (-) = 11
No biochemical or clinical recurrence (n = 45)	Median: 65 Mean: 63.5 Range: 40-75	Median: 6.0 Mean: 7.9 Range: 0.5 - 23	T1 C = 24 T2 A = 6 T2 B = 15	5 = 8 6 = 9 7 = 22 8 = 6	(+) = 6 (-) = 39	(+) = 10 (-) = 35	(+) = 3 (-) = 42

Table 2: Sensitivity, specificity, accuracy, PPV and NPV of HA, HYAL1 and combined HA-HYAL1 staining inferences for predicting biochemical recurrence in CaP patients. Note that 64 month follow-up was used a cut point for determining biochemical recurrence. Please note that 2 of the CaP patients who had a biochemical recurrence at 70 months and showed high-grade HA, HYAL1 and combined HA-HYAL1 staining were considered as false-positives and were included in the specificity calculation.

Parameters	HA	HYAL1	HA-HYAL1
Sensitivity	96% (24/25)	84% (21/25)	84% (21/25)
Specificity	55.5% (25/45)	82.2% (37/45)	86.7% (39/45)
Accuracy	70% (49/70)	82.9% (58/70)	85.7% (60/70)
PPV	54.5% (24/44)	70% (21/30)	77.8% (21/27)
NPV	96.2% (25/26)	90.2% (37/41)	90.7% (39/43)

Table 3: Univariate analysis of pre- and post-operative prognostic parameters and HA, HYAL1 and combined HA-HYAL1 staining inferences. *: Statistically significant. CI: Confidence Interval.

Parameter	*Chi* square	P value	Odds Ratio	95% CI
Age	1.088	0.297	1.041	0.965 – 1.122
PSA	5.652	0.0174*	1.1	1.017 – 1.192
Clinical stage	0.539	0.287	1.741	0.636 – 4.621
Gleason sum (Overall)	9.266	0.0023*	3.062	1.49 – 6.294
Gleason sum ≥ 7	5.919	0.015*	6.982	1.459 – 33.411
Margin	14.764	0.0001*	9.0	2.934 – 27.603
EPE	25.435	< 0.0001*	34.125	8.655 – 134.545
Seminal vesicle invasion	15.969	< 0.0001*	17.818	4.339 – 73.175
HA	10.222	0.0014*	30.0	3.729 – 241.337
HYAL1	22.627	< 0.0001*	24.281	6.524 – 90.375
HA-HYAL1	25.435	< 0.0001*	34.125	8.655 – 134.545

Table 4: Forward stepwise multiple logistic regression analysis of pre- and post-operative prognostic parameters and HA, HYAL1 and combined HA-HYAL1 staining inferences. The significant parameters ($P > 0.05$) selected by the model are shown. **A:** In the analysis, HA and HYAL1staining inferences were included separately, along with other pre- (i.e., age, PSA and clinical stage) and post- (i.e., Gleason sum (or stratified Gleason as ≥ 7 and < 7), EPE, margin +/-, and seminal vesicle invasion) surgery parameters. **B:** Combined HA-HYAL1 staining inference was included in the analysis together with the above-mentioned pre- and post-operative parameters. NA: Not applicable. *: Statistically significant.

Table 4 A					**Table 4 B**			
Parameter	*Chi* Square	P value	Odds Ratio	95% CI	*Chi* Square	P value	Odds Ratio	95% CI
EPE	15.20	0.0023*	33.483	3.493 – 320.912	9.271	0.0023*	35.944	3.583 – 360.565
Margin	7.573	0.0059*	26.948	2.58 – 281.463	6.895	0.0086*	24.438	2.249 - 265.55
HYAL1	6.846	0.0094*	12.423	1.856 – 83.158	NA	NA	NA	NA
HA-HYAL1	NA	NA	NA	NA	8.628	0.0033*	18.047	2.619 – 124.378

FIGURE LEGENDS:

Figure 1. HA staining of CaP specimens from non-progressed and progressed patients. HA was localized in CaP tissues using a biotinylated HA-binding protein and a streptavidin peroxidase DAB-chromogen detection system. Panels A, C and E: HA staining in specimens from non-progressed patients. Panels B, D and F: HA staining in specimens from progressed patients. A, B: Gleason 6 CaP; C, D: Gleason 7 CaP; E, F: Gleason 8 CaP.

Figure 2: A Gleason 8 CaP specimen with tumor cells showing HA staining. Gleason 8 specimen from a progressed patient where tumor cells show high-grade HA staining. A: 100 X magnification. B: 400 X magnification.

Figure 3: HYAL1 staining of CaP specimens from non-progressed and progressed patients. HYAL1 was localized in CaP tissues using an anti-HYAL1 antibody and a streptavidin peroxidase DAB-chromogen detection system. Panels A, C and E: HYAL1 staining in specimens from non-progressed patients. Panels B, D and F: HYAL1 staining in specimens from progressed patients. A, B: Gleason 6 CaP; C, D: Gleason 7 CaP; E, F: Gleason 8 CaP.

Figure 1

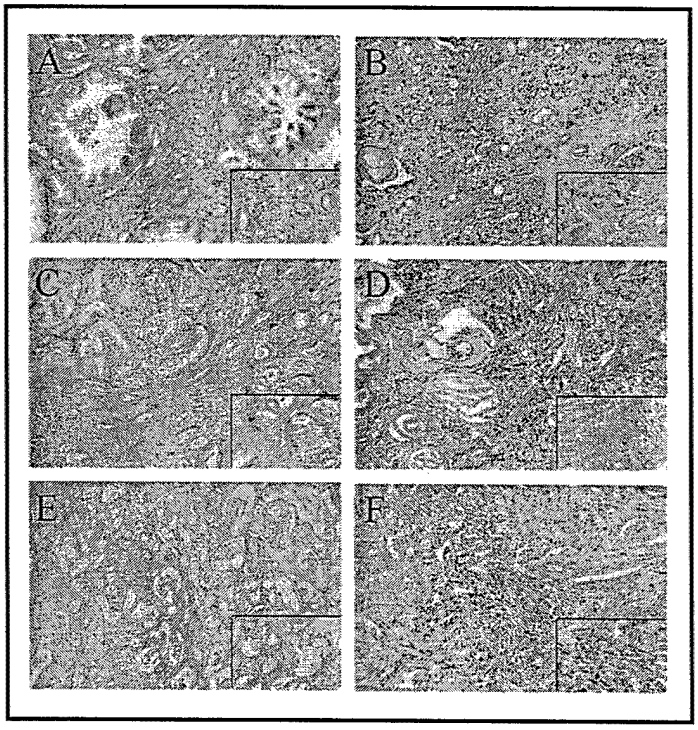

Figure 2

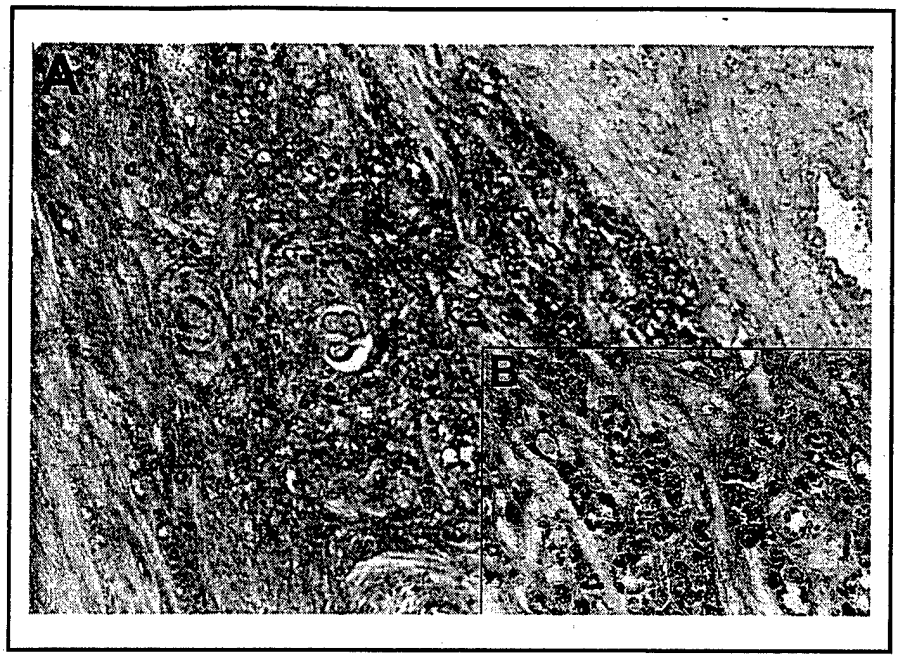

Figure 3